

UMAP

**Modules in
Undergraduate
Mathematics
and Its
Applications**

**Published in
cooperation with**

**The Society for
Industrial and
Applied Mathematics,**

**The Mathematical
Association of America,**

**The National Council
of Teachers of
Mathematics,**

**The American
Mathematical
Association of
Two-Year Colleges,**

**The Institute for
Operations Research
and the Management
Sciences, and**

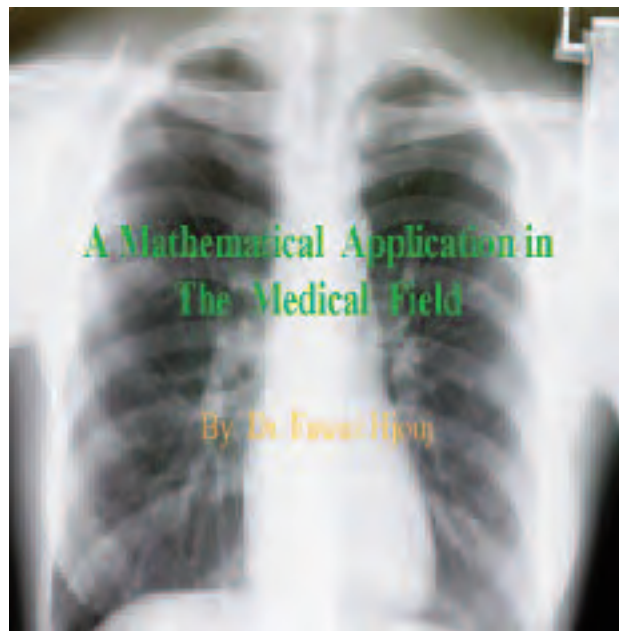
**The American
Statistical Association.**

The logo for COMAP, consisting of the letters 'COMAP' in a stylized, cursive, black font.

Module 794

The Mathematics of Medical X-Ray Imaging

Fawaz Hjouj
Dept. of Mathematics
East Carolina University
Greenville, NC 27858
hjouj@ecu.edu



**Numerical Analysis,
Fourier Analysis**

INTERMODULAR DESCRIPTION SHEET:	UMAP Unit 794
TITLE:	The Mathematics of Medical X-Ray Imaging
AUTHOR:	Fawaz Hjouj Dept. of Mathematics East Carolina University Greenville, NC 27858 hjoujf@ecu.edu
MATHEMATICAL FIELD:	Numerical analysis, Fourier analysis
APPLICATION FIELD:	Medicine
TARGET AUDIENCE:	Students in the mathematical, physical, and engineering sciences
ABSTRACT:	Determining the internal structure of an object without having to cut it, or viewing a section of a body without interference from other regions, have long been goals of radiologists and engineers. These goals have been achieved through computed tomography (CT) and other technologies that are used in every hospital. This Module on CT should help readers appreciate this technology and the underlying mathematics.
PREREQUISITES:	The usual core courses in calculus/physics; experience in the use of Matlab or a similar program is a plus.

UMAP/ILAP Modules 2006: Tools for Teaching, 87–130.
©Copyright 2006 by COMAP, Inc. All rights reserved.

Permission to make digital or hard copies of part or all of this work for personal or classroom use is granted without fee provided that copies are not made or distributed for profit or commercial advantage and that copies bear this notice. Abstracting with credit is permitted, but copyrights for components of this work owned by others than COMAP must be honored. To copy otherwise, to republish, to post on servers, or to redistribute to lists requires prior permission from COMAP.

COMAP, Inc., Suite 3B, 175 Middlesex Tpke., Bedford, MA 01730
(800) 77-COMAP = (800) 772-6627, or (781) 862-7878; <http://www.comap.com>

The Mathematics of Medical X-Ray Imaging

Fawaz Hjouj
Dept. of Mathematics
East Carolina University
Greenville, NC 27858
hjoujf@ecu.edu

Table of Contents

1. ABOUT THIS MODULE	1
2. THE BIG IDEA (RECONSTRUCTION)	2
3. BASICS OF X-RAY	2
4. BASIC CONCEPTS	5
5. THE FOURIER TRANSFORM	8
6. PROJECTIONS	11
7. MORE ON PROJECTIONS	15
8. RECONSTRUCTION	19
8.1 An Old Idea (Back Projection)	21
9. A GLIMPSE OF COMPUTED TOMOGRAPHY	25
10. FILTERED BACK PROJECTION	26
11. MATLAB PROJECT	32
12. SOLUTIONS TO THE EXERCISES	36
REFERENCES	40

ABOUT THE AUTHOR 40

MODULES AND MONOGRAPHS IN UNDERGRADUATE
MATHEMATICS AND ITS APPLICATIONS (UMAP) PROJECT

The goal of UMAP is to develop, through a community of users and developers, a system of instructional modules in undergraduate mathematics and its applications, to be used to supplement existing courses and from which complete courses may eventually be built.

The Project was guided by a National Advisory Board of mathematicians, scientists, and educators. UMAP was funded by a grant from the National Science Foundation and now is supported by the Consortium for Mathematics and Its Applications (COMAP), Inc., a nonprofit corporation engaged in research and development in mathematics education.

Paul J. Campbell
Solomon Garfunkel

Editor
Executive Director, COMAP

1. About This Module

This Module is part of an effort to create simplified elementary introductions to interesting applications of undergraduate mathematics for students from diverse fields, such as mathematics, engineering sciences, and others.

The central idea of this Module is that we can determine the internal structure of an object without having to cut the object. In other words, we can reconstruct a function defined on a region, by using its line integral.

Students in the mathematical, physical, or engineering sciences will find it interesting how basic elements of mathematics, such as the concepts of functions of two variables, lines, integrals, numerical integration, polar systems, and other concepts, are used in a very definite, useful application in life.

Here are some remarks for students and instructors to consider:

- We assume that students have mastered calculus, including calculus of functions of two variables.
- To practice the ideas of the subject and to solve most of the exercises that we include, knowledge of the basics of the computer algebra system Matlab is needed. Getting started with Matlab is easy, especially with some minimal help from an instructor. In addition, by solving the exercises in this Module, students not only learn the concepts more deeply but also enhance skills in Matlab. Indeed, the last section of this Module is an interesting project where we show students how to recover an image of their choice.
- This Module is prepared to fit the undergraduate student. However, some known concepts are treated through approaches that are different from the usual calculus style. For example, we have a different look at the line integral of a function, and we think that it would be a good exercise for students to make the connection between this approach and the standard calculus approach of defining the line integral using parametric equations.
- The Fourier transform and related subjects are normally not treated in the calculus sequence. We treat the very basics of this subject in **Section 5** and include some examples and exercises for students to solve. This section is needed if students want to follow the derivation in **Section 10**. Students who skip the difficult steps in **Section 10** and accept the results (**24–26**) stated on p. 28 can skip **Section 5** as well. However, we recommend that students majoring in mathematics give this study sufficient effort to learn the necessary details.

In addition, there are a few places where derivations are beyond the stated prerequisites, which is not unusual.

2. The Big Idea (Reconstruction)

When sunshine (a probe) hits my body (an object), the shadow (profile) of my body is formed on the ground. Further, if you cannot see me but are able to see my shadow, you would have some rough idea about whose shadow it is.

A large class of reconstruction problems from medicine, astronomy, geophysics, molecular biology, and many other fields are united in the frame of this three-step big idea:

1. Act on the unseen structure of an object (human brain, an engine, a bag, etc.) by some probe (x-ray, gamma rays, etc.).
2. Detect the probe (by collecting data) to produce profiles (projections).
3. Explore the profiles by mathematical tools to identify the internal structure.

We will use the term projections for profiles. **Figure 1** explains the idea.

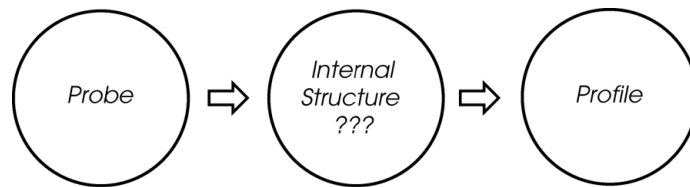


Figure 1. Internal distribution is acted on by probes to produce profiles.

3. Basics of X-Ray

A favorite experiment among physicists in the mid-1890s was to send currents through small, pear-shaped glass tubes under various conditions, as shown in **Figure 2**. The German physicist Wilhelm Conrad Roentgen (1845–1923) discovered x-rays in 1895 while performing similar experiments in a completely darkened room. It was a surprise to him to find out that whenever the tube was energized, a soft glow was produced on a cardboard-coated phosphor that lay on a chair a few feet away [Kevles 1997].

What occurred is that a beam of electrons, accelerated by a very high voltage in the tube, struck the target (anode) and x-rays were produced. Roentgen was even more surprised when he began to measure the brightness of this glow. By holding his own hand in the path of the rays, he saw an outline of his living bones. He named these mysterious new rays *x-rays*.

It did not take him long to carry out more investigations of this discovery. He recorded the following:

- An x-ray beam can penetrate, be partially attenuated, but also travel through a thickness of solid material.

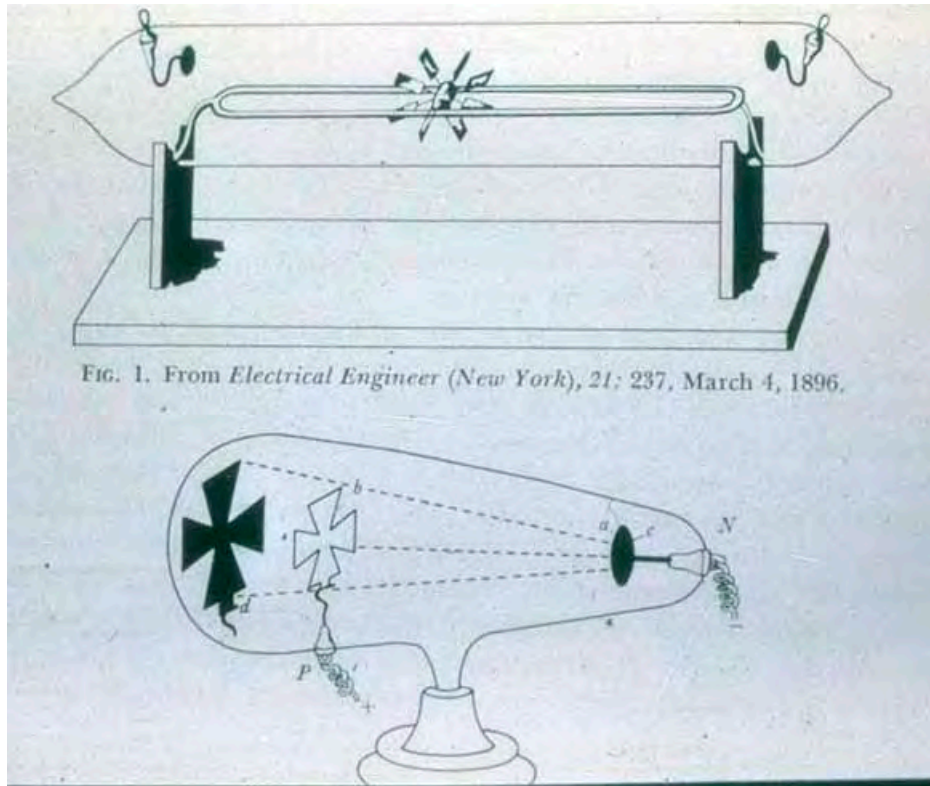


FIG. 1. From *Electrical Engineer (New York)*, 21: 237, March 4, 1896.

Figure 2. Early experimental tubes like those used by Roentgen and others to investigate the nature of light. (Courtesy of Radiology Centennial, Inc.)

- The transmitted x-rays can sensitize a photographic film to produce a visible image. Indeed, Roentgen obtained the first radiographic image, of his wife's hand (**Figure 3**) [Kevles 1997].

Roentgen was awarded the first Nobel Prize for Physics for his discovery of x-rays. In the years following, physicists found that x-rays were just a new member of the *electromagnetic spectrum*, a term used to describe many types of radiation (see **Figure 4**). Physicists also showed that an x-ray is electromagnetic radiation with high frequency (10^{17} – 10^{20} Hz) and short wavelength (10^{-9} m).

Two of the best-known applications of x-rays in the medical field are:

- Conventional x-ray imaging, which is made by allowing the x-rays to diverge from a source, pass through the body of the subject, and then fall on a sheet of photographic film. Although modern conventional imaging equipment is highly developed, the method of producing x-rays is still the same as used by Roentgen himself.
- Computed tomography (CT), which allows for complete exclusion of sections not under study. In this method, the x-ray passes through the desired plane of the body without entering other areas. Projections of the radiations detected at different angles are used with a computer to reconstruct the structure in question.



Figure 3. The famous radiograph made by Roentgen on 22 December 1895. This is traditionally known as “the first X-ray picture” and “the radiograph of Mrs. Roentgen’s hand.” (Courtesy of Radiology Centennial, Inc.)

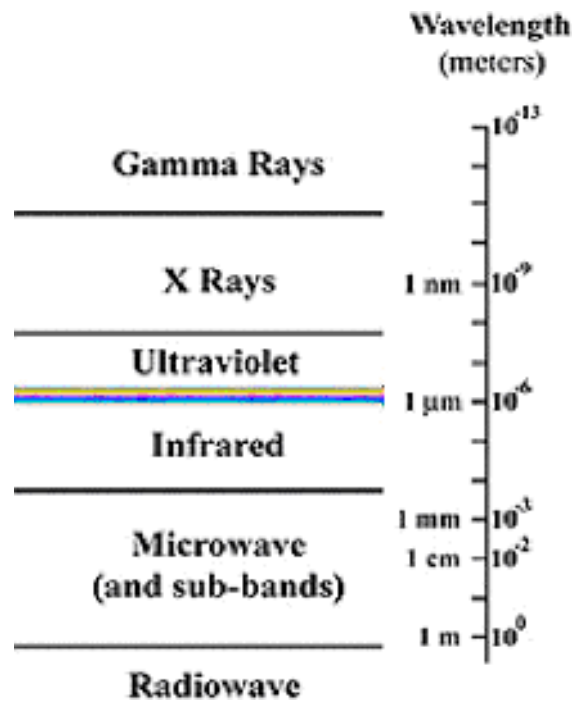


Figure 4. The electromagnetic spectrum.

In this Module, we explore the mathematics used in CT. **Figures 5ab** show conventional x-ray vs. reconstructive tomography.

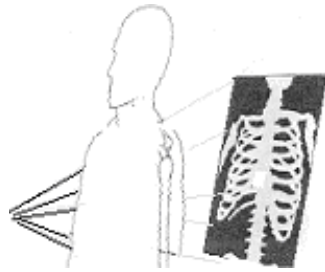


Figure 5a. Production of a radiographic image by forming an x-ray shadowgram.

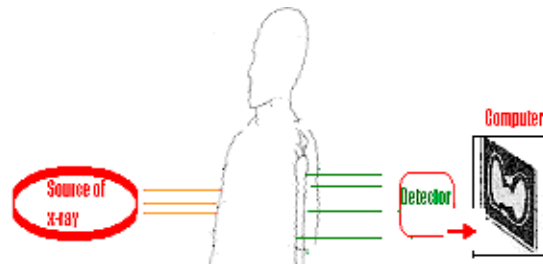


Figure 5b. Computer tomography (CT).

4. Basic Concepts

Given a suitably regular function $f(x, y)$ on the plane \mathbb{R}^2 , one way to represent f is by the usual display of the surface generated by this function. **Example 1** illustrates the idea.

Example 1: Unit box Let

$$f(x, y) := \text{box}(x, y) := \begin{cases} 1, & \text{if } |x| \leq \frac{1}{2} \text{ and } |y| \leq \frac{1}{2}; \\ 0, & \text{otherwise.} \end{cases} \quad (1)$$

We will often use this particular function throughout and wish to call it “the box function” or simply $b(x, y)$. **Figure 6a** displays the surface plot of this box function. An alternative display of this function can be via a density plot, as shown in **Figure 6b**.

Indeed, an image can be defined as a function $f(x, y)$ where the value of f at any pair (x, y) is called the *intensity* or *gray level* of the image at that point. When x, y , and $f(x, y)$ are all discrete quantities, we call the image a *digital image*. A digital image is composed of elements, each with a particular location and value, called *picture elements* or *pixels* [Gonzales and Woods 2002]. In this way, **Figure 6b** is the digital image defined by the function $b(x, y)$. For deeper understanding, we recommend that you practice these ideas on a computer. All images in this Module were generated using Matlab. For instance, the Matlab code in **Table 1** generates **Figures 6a** and **6b**.

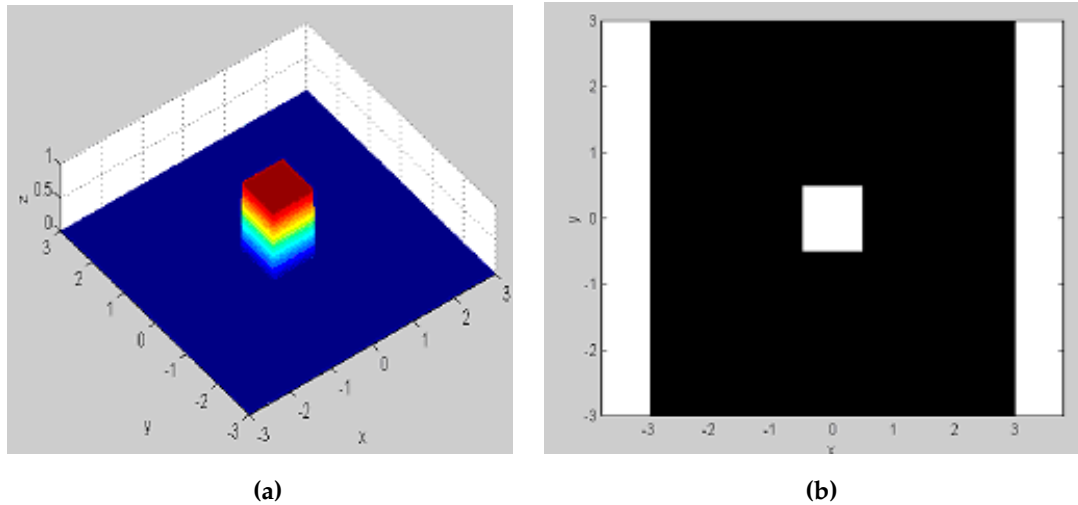


Figure 6. Representation of the unit box: (a) by a surface; (b) by a density plot.

Exercise

1. Use Code1 on p. 7 to display a representation of the radially symmetric Gaussian

$$f(x, y) := e^{-(x^2+y^2)},$$

- a) by a surface;
- b) by a density plot.

Since we will use the concept of line integral, we introduce a formula for specifying a line L . Usually, a line is given by the equation $y = mx + b$. Instead, we use real coordinates p, ϕ such that

$$L_{\phi,p} = \{(x, y) \in \mathbb{R}^2 : x \cos \phi + y \sin \phi = p\}. \quad (2)$$

As shown in **Figure 7**, a ray through the origin at angle ϕ is perpendicular to this line and p is the signed distance from the origin to this line.

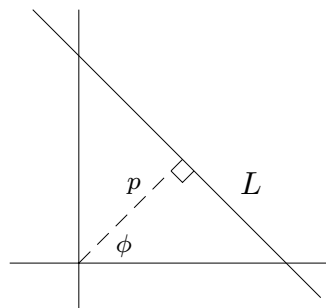


Figure 7. The line (2) specified by the coordinates p, ϕ .

Table 1. Code1.

```

% Code1: a script MATLAB file; generates surface
% and density plots for the symmetric unit Box.

step = .03;
s = -3:step:3;  t=s;

[A,B]= meshgrid(s,t);          % define a grid
C = zeros(length(s),length(s));
for i=1:length(s)
for j=1:length(t)
    x=A(i,j);
    y=B(i,j);
    if abs(x)<=1/2 & abs(y)<=1/2
        C(i,j)= 1;
    else
        C(i,j)= 0;
    end
end
end
end
figure(1)
surf(A,B,C)                    % display the surface
view([20,20,120])
shading interp
xlabel('x')
ylabel('y')
zlabel('z')
title('Surface of the Box Function')

figure(2)
pcolor(A,B,C)                  % display the image
colormap(gray);
shading interp
xlabel('x')
ylabel('y')
axis equal
title('Density Plot for the Box Function')

```

Exercise

2. Prove that any point (x, y) on the line L satisfies the equation given in (2), i.e.,

$$x \cos \phi + y \sin \phi = p.$$

5. The Fourier Transform

An integral transform is a relation of the form

$$F(s) = \int_a^b f(x)k(s, x) dx,$$

where a given function f is transformed into the function F by means of the integral. The function F is said to be the *transform* of f , and the function k is called the *kernel*. By making a suitable choice of the kernel and the integration limits a and b , we produce different transforms. Indeed, several integral transformations are widely used, among which is the *Fourier transform*

$$F(s) = \int_{x=-\infty}^{\infty} f(x)e^{-2\pi isx} dx, \quad -\infty < s < \infty. \quad (3)$$

Here the function f is defined on the real line \mathbb{R} , and the complex exponential $e^{2\pi isx}$ can be written as

$$e^{2\pi isx} := \cos(2\pi sx) + i \sin(2\pi sx), \quad \text{where } i^2 = -1.$$

Remark. We sometimes use the term *Fourier transform operator* \mathcal{F} and write

$$(\mathcal{F}f)(s) = F(s).$$

One of the big ideas behind the use of the transform is that we can transform a problem for f into a problem for F , which is sometimes a simpler problem; if so, we solve the simpler problem and then recover the desired function f from its transform F .

Fourier discovered that a function f defined on the real line can be synthesized using the transform F :

$$f(x) = \int_{s=-\infty}^{\infty} F(s)e^{2\pi isx} ds, \quad -\infty < x < \infty. \quad (4)$$

We purposefully will not consider the exact hypotheses that guarantee the existence of such a Fourier representation. Roughly speaking, the Fourier representation (4) is possible in all cases where f does not fluctuate too widely

and where the tails of f at $\pm\infty$ are not too large. We refer to (4) as the *synthesis equation* and to (3) as the *analysis equation* for f [Kammler 2000, 3].

In practice, it is not easy to find the transform from the definition. A special calculus was developed for finding Fourier transforms for commonly used functions on \mathbb{R} . Kammler argued “that we need to memorize a few Fourier transform pairs f, F and learn certain rules for modifying or combining known pairs to obtain new ones” [2000].

Example 2: The sinc function The function

$$f(x) = \begin{cases} 1, & \text{if } -\frac{1}{2} < x < \frac{1}{2}; \\ 0, & \text{otherwise,} \end{cases}$$

and its Fourier transform

$$F(s) = \text{sinc}(s) := \frac{\sin(\pi s)}{\pi s} \tag{5}$$

are two of the most commonly used functions in Fourier analysis [Kammler 2000, 130]. **Figure 8** shows the graphs of both $f(x)$ and $F(s)$.

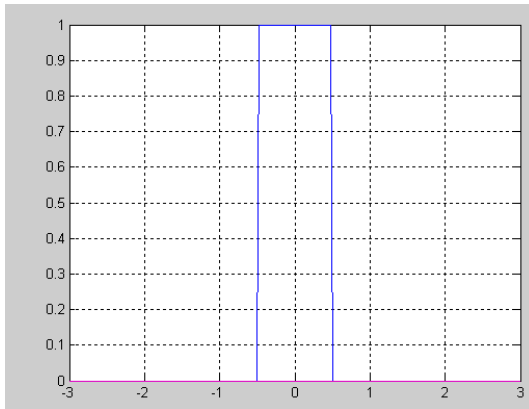


Figure 8a. The graph (i.e., the line at the top!) of the function $f(x)$ from **Example 2**.

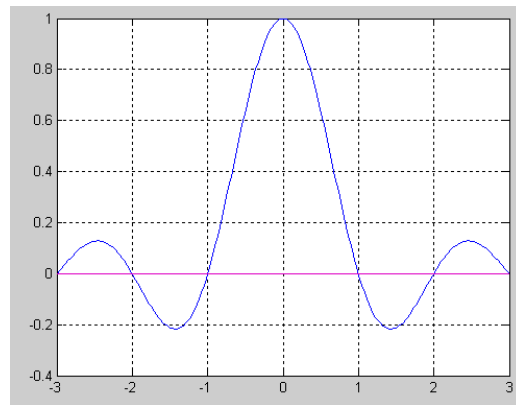


Figure 8b. The graph of the function $F(s)$ from **Example 2**.

Exercise

- Let $f(x) = e^{-\pi x^2}$, which is usually called the *unit gaussian*. Use the fact that f is an even function to prove that

$$F(s) = e^{-\pi s^2}.$$

In the same way, the Fourier transform of the function $f(x, y)$ defined on \mathbb{R}^2 is

$$F(u, v) = \int_{x=-\infty}^{\infty} \int_{y=-\infty}^{\infty} f(x, y) e^{-2\pi i(ux+vy)} dy dx, \tag{6}$$

with

$$f(x, y) = \int_{u=-\infty}^{\infty} \int_{v=-\infty}^{\infty} F(u, v) e^{2\pi i(ux+vy)} dv du. \quad (7)$$

We can use univariate methods to evaluate these bivariate integrals when f is separable in x, y coordinates; that is, when f is a product,

$$f(x, y) = f_1(x) \cdot f_2(y),$$

we can show that

$$F(u, v) = F_1(u) \cdot F_2(v), \quad (8)$$

where F_1 and F_2 are the univariate Fourier transforms of f_1, f_2 .

Exercise

4. Prove (8).

Example 3: Fourier transform of a function of two variables Let us find the Fourier transform of the function

$$f(x, y) = \begin{cases} 1, & \text{if } |x| < \frac{1}{2}, \quad |y| < \frac{1}{2}; \\ 0, & \text{otherwise} \end{cases}$$

We observe that

$$f(x, y) = f_1(x) \cdot f_2(y) \quad \text{with}$$

$$f_1(x) = \begin{cases} 1, & \text{if } |x| < \frac{1}{2}; \\ 0, & \text{otherwise,} \end{cases}$$

and

$$f_2(y) = \begin{cases} 1, & \text{if } |y| < \frac{1}{2}; \\ 0, & \text{otherwise.} \end{cases}$$

Thus,

$$\begin{aligned} F(u, v) &= F_1(u) \cdot F_2(v) && \text{(using (8))} \\ &= \text{sinc}(u) \cdot \text{sinc}(v) && \text{(using (5)).} \end{aligned}$$

Figure 9 shows the graph of $f(x, y)$ and its Fourier transform $F(u, v)$.

Exercise

5. Find the Fourier transform of the unit gaussian

$$f(x, y) := e^{-\pi(x^2+y^2)}.$$

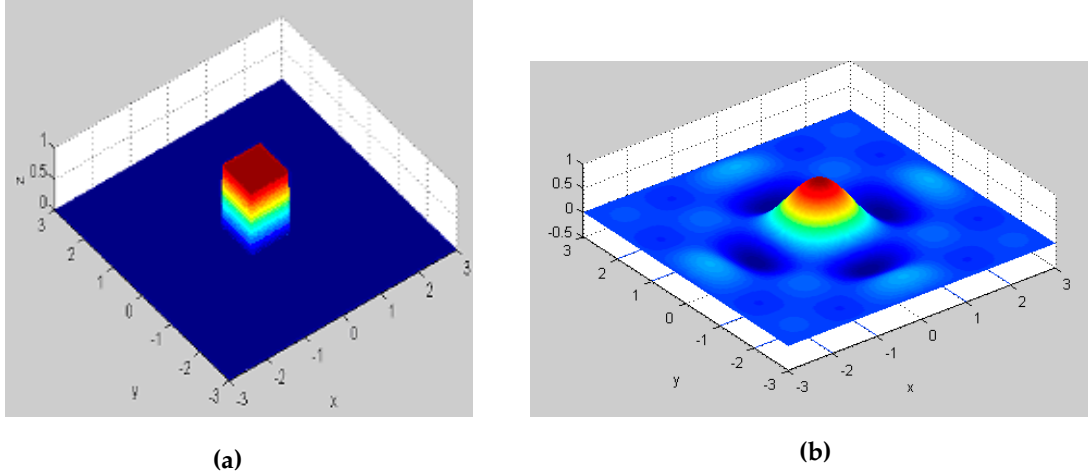


Figure 9. **a.** The graph of $f(x, y)$. **b.** Its Fourier transform $F(u, v)$ from Example 3.

6. Projections

Given a suitably regular real valued function f on the plane \mathbb{R}^2 , we define the profiles (projections):

$$f^\vee\{L\} := \int_L f(x, y) ds, \tag{9}$$

where ds is the differential of arc length along a line L from the set of lines L on \mathbb{R}^2 . In other words, $f^\vee\{L\}$ is the line integral of $f(x, y)$ along the line L .

In 1917, J. Radon showed that it is possible to recover f from the set of projections (9) when f is a continuous function with compact support. (An English translation of his paper is given in Deans [1983]). The projection $f^\vee\{L\}$ is also called the *Radon transform* of the function f .

A nice elementary introduction to the Radon transform and its applications is given in Deans [1983]. Bracewell [1986] gives many practical insights for working with the Radon transform in image processing. The advanced engineering text by Z.P. Liang and the 2003 Nobel Laureate P.C. Lauterbur summarizes the basic concepts needed for understanding modern MRI imaging [1999].

It is more convenient to denote

$$f^\vee\{L\} := f_\phi^\vee(p),$$

where p, ϕ are the parameters of L as given in (2). We get all possible lines by taking $-\infty < p < \infty$ and $0 \leq \phi < \pi$.

For some angle, say $\phi = \phi_0$, $f_{\phi_0}^\vee(p)$ is a single number equal to the line integral of $f(x, y)$ along the line $L_{\phi_0, p}$. Thus, the profile $f_{\phi_0}^\vee(p)$ is a function of one variable, namely p . In this way, we see that to every ϕ we can define the profile $f_\phi^\vee(p)$.

The following two examples illustrate the idea.

Example 4: Radon transform of the box function Consider the box function

$$f(x, y) := \text{box}(x, y) := \begin{cases} 1, & \text{if } |x| \leq \frac{1}{2} \text{ and } |y| \leq \frac{1}{2}; \\ 0, & \text{otherwise.} \end{cases}$$

as in **Example 1**. We wish to explore the profiles that correspond to $\phi = 0^\circ$, 45° , i.e., $b_0^\vee(p)$ and b_{45}^\vee . Notice that $L_{0,p}, p \in \mathbb{R}$ is a family of vertical lines, as shown in **Figure 10a**, and $b(x, y)$ takes constant values of either 0 or 1 when (x, y) is outside or inside the support square. Thus, the line integral $\int b(x, y) ds$ along any line L of this family is the length of the line segment that lies within the square shown in **Figure 10b**. For instance, $b_0^\vee(0) = b_0^\vee(\frac{1}{2}) = b_0^\vee(-\frac{1}{2}) = 1$, and $b_0^\vee(.6) = b_0^\vee(-.6) = 0$. **Figure 10b** also displays the graph of $b_0^\vee(p)$ where p is on the horizontal axis and $b_0^\vee(p)$ is on the vertical axis. Therefore, the function (profile) $b_0^\vee(p)$ of the box function can be described by:

$$b_0^\vee(p) = \begin{cases} 1, & -\frac{1}{2} \leq p \leq \frac{1}{2}; \\ 0, & \text{otherwise.} \end{cases}$$

As for the case $\phi = 45^\circ$, the profile $b_{45^\circ}^\vee(p)$ is shown in **Figure 10c**. We recommend that you make sense of this profile just by intuitive thinking. However, a complete derivation of $b_\phi^\vee(p)$ for the box function is given in the next section.

Example 5: Unit cylinder Let

$$f(x, y) := \begin{cases} 1, & \text{if } x^2 + y^2 \leq (\frac{1}{2})^2; \\ 0, & \text{otherwise.} \end{cases} \quad (10)$$

This function takes the value 1 at any point (x, y) inside the circle $x^2 + y^2 \leq (\frac{1}{2})^2$ and 0 outside, as shown in **Figure 11ab**.

Figure 11c displays rough plots of four profiles corresponding to the angles $\phi = 0^\circ, 45^\circ, 90^\circ$, and 135° . We retain this example for more formal work later in this paper.

Exercise

- Given the binary image (T) that corresponds to some function $f(x, y)$ as shown in **Figure 12**, sketch (by hand) rough graphs of $f_0^\vee(p)$ and $f_{90}^\vee(p)$.

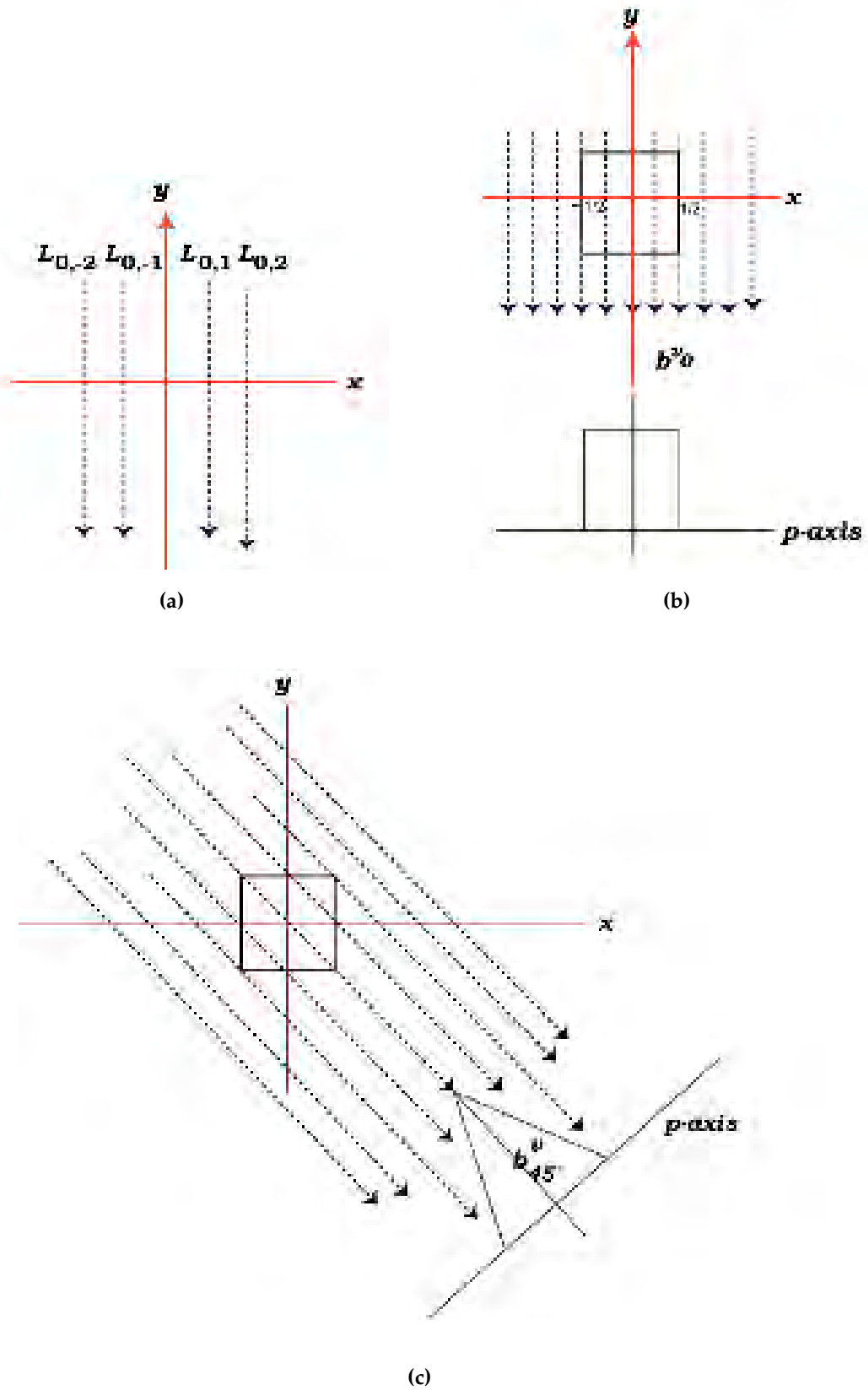
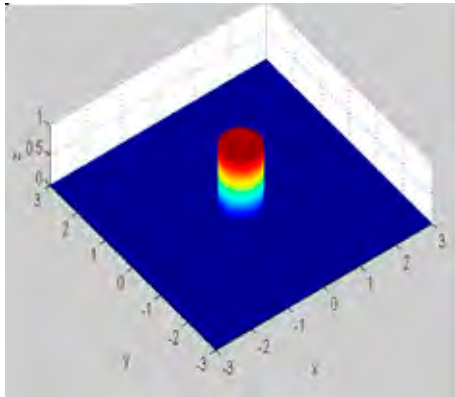
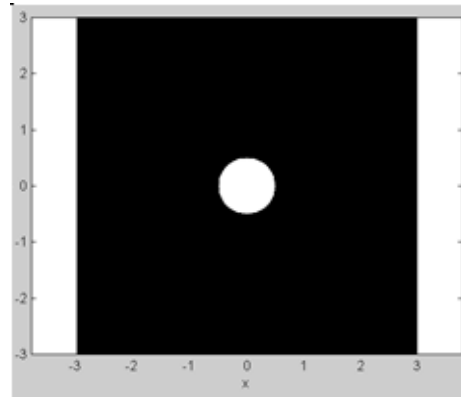


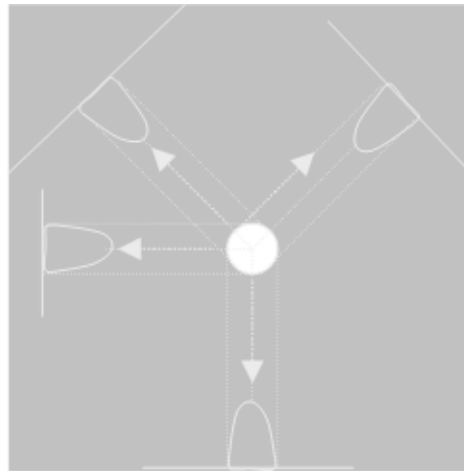
Figure 10. a. Lines $L_{0,-2}, L_{0,-1}, L_{0,1}, L_{0,2}$. b. The graph b^y_0 of the box function. c. The graph b^{45}_y of the box function.



(a)



(b)



(c)

Figure 11. a, b. Representation of the symmetric unit cylinder (10) by a surface and by a density plot. c. Rough plots for the profiles $f_{0^\circ}^V$, $f_{45^\circ}^V$, $f_{90^\circ}^V$, $f_{135^\circ}^V$ for the unit cylinder.

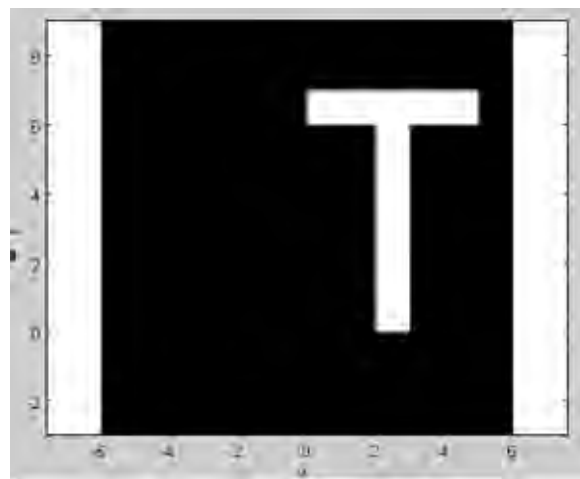


Figure 12. The T image.

7. More on Projections

We now know that the profile $f_\phi^\vee(p)$ of $f(x, y)$ corresponding to the angle ϕ is given by

$$f_\phi^\vee(p) = \int_L f(x, y) ds.$$

We can find a practical formula to evaluate $f_\phi^\vee(p)$. In fact, if $\phi = 0$, then the $L_{0,p}$ are vertical lines and

$$f_0^\vee(p) = \int_{-\infty}^{\infty} f(p, y) dy \text{ (integrating along vertical lines).}$$

On the other hand, if $\phi = \frac{\pi}{2}$, then then $L_{(\pi/2),p}$ are horizontal lines and

$$f_{\pi/2}^\vee(p) = \int_{-\infty}^{\infty} f(x, p) dx \text{ (integrating along horizontal lines).}$$

More generally, if we let $x = p \cos \phi - s \sin \phi$ and $y = p \sin \phi + s \cos \phi$, then

$$f_\phi^\vee(p) = \int_{-\infty}^{\infty} f(p \cos \phi - s \sin \phi, p \sin \phi + s \cos \phi) ds. \quad (11)$$

We will have occasion to evaluate integrals of the form (11), and this process is facilitated by a number of rules [Deans 1983; Liang and Lauterbur 1999]. In particular, we need the following two rules:

Let f_1, f_2 be suitably regular functions on \mathbb{R}^2 , and let c_1, c_2, x_0, y_0 be real scalars:

(a) *Linearity rule:*

$$\begin{aligned} \text{If } g(x, y) &= c_1 f_1(x, y) + c_2 f_2(x, y), \text{ then} \\ g_\phi^\vee(p) &= c_1 f_{1,\phi}^\vee(p) + c_2 f_{2,\phi}^\vee(p). \end{aligned} \quad (12)$$

Exercise

7. Prove rule (12).

(b) *Translation rule:*

$$\begin{aligned} \text{If } g(x, y) &= f(x - x_0, y - y_0), \text{ then} \\ g_\phi^\vee(p) &= f_\phi^\vee[p - (x_0 \cos \phi + y_0 \sin \phi)]. \end{aligned} \quad (13)$$

We now compute the Radon projections for several elementary functions.

Example 6: Radon transform of the unit cylinder Let

$$f(x, y) := \begin{cases} 1, & \text{if } x^2 + y^2 \leq \left(\frac{1}{2}\right)^2; \\ 0, & \text{otherwise.} \end{cases}$$

By symmetry, we can write $f_\phi^\vee(p) = f_0^\vee(p)$.

Using (11) with $\phi = 0$, we find:

$$\begin{aligned} f_\phi^\vee(p) &= f_0^\vee(p) = \int_{-\infty}^{\infty} f(p, y) dy \\ &= \begin{cases} \int_{-\sqrt{(1/4)-p^2}}^{\sqrt{(1/4)-p^2}} dy, & \text{if } |p| < \frac{1}{2}; \\ 0, & \text{otherwise;} \end{cases} \quad (14) \\ &= \begin{cases} \sqrt{1-4p^2}, & \text{if } |p| < \frac{1}{2}; \\ 0, & \text{otherwise.} \end{cases} \end{aligned}$$

Figure 13 illustrates this example.

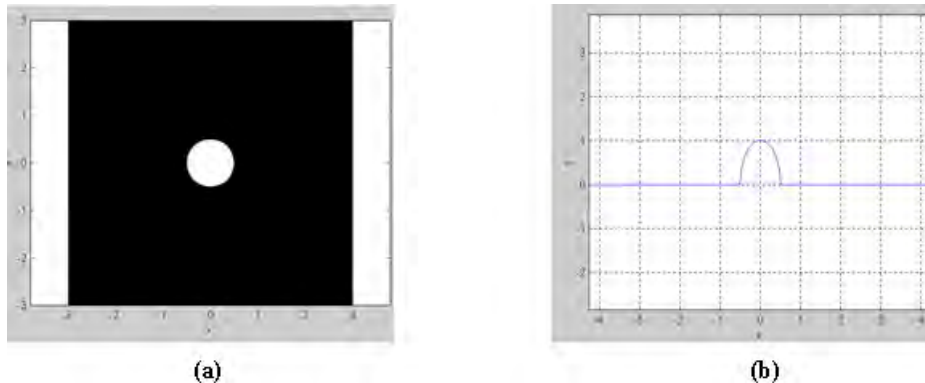


Figure 13. Representations of the radially symmetric unit cylinder by a density plot (a) and by the profile f_0^\vee (b).

Example 7: Radon transform of the unit box Let

$$f(x, y) := \text{box}(x, y) := \begin{cases} 1, & \text{if } |x| \leq \frac{1}{2} \text{ and } |y| \leq \frac{1}{2}; \\ 0, & \text{otherwise.} \end{cases}$$

We find $f_\phi^\vee(p)$ for $0 \leq \phi \leq \frac{\pi}{4}$, and then make use of symmetry. Given $0 \leq \phi \leq \frac{\pi}{4}$, we divide the plane into five regions using lines through the corners of the box as shown in **Figure 14**. Since $f(x, y)$ takes the constant value 1 (respectively, 0) when (x, y) is inside (respectively, outside) the support square, $f_\phi^\vee(p) = \int_L f(x, y) ds$ is just the length of the segment of the line L that lies within the square.

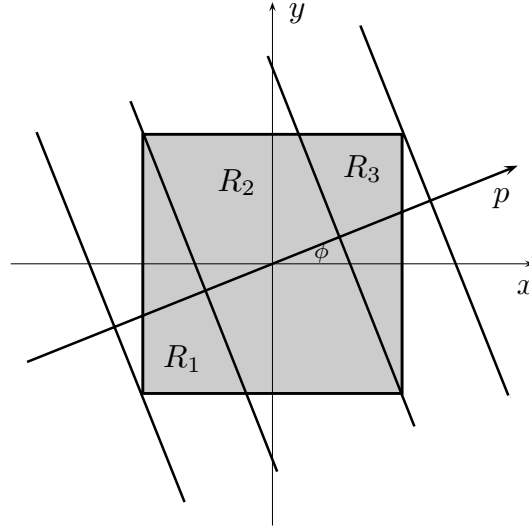


Figure 14. Regions of the unit box used to obtain (15).

This being the case, we can use elementary trigonometry to write

$$f^\vee(p, \phi) = \begin{cases} \frac{\sin \phi + \cos \phi - 2p}{2 \sin \phi \cos \phi}, & \text{if } \frac{1}{2} \cos \phi - \frac{1}{2} \sin \phi \leq p \\ & \leq \frac{1}{2} \cos \phi + \frac{1}{2} \sin \phi; \\ \frac{1}{\cos \phi}, & \text{if } 0 \leq |p| \leq \frac{1}{2} \cos \phi - \frac{1}{2} \sin \phi; \\ \frac{\sin \phi + \cos \phi + 2p}{2 \sin \phi \cos \phi}, & \text{if } -\frac{1}{2} \cos \phi - \frac{1}{2} \sin \phi \leq p \\ & \leq -\frac{1}{2} \cos \phi + \frac{1}{2} \sin \phi; \\ 0, & \text{otherwise.} \end{cases} \quad (15)$$

When $-\pi \leq \phi \leq \pi$, we replace ϕ by $\min\{|\phi|, \pi - |\phi|, |\frac{\pi}{2} - |\phi||\}$ and then use (15) with this new argument. We illustrate this example in Figure 15.

Example 8: Radon transform of the letter F Let

$$\begin{aligned} f(x, y) := & b\left(x - \frac{1}{2}, y - \frac{1}{2}\right) + b\left(x - \frac{1}{2}, y - \frac{3}{2}\right) + b\left(x - \frac{1}{2}, y - \frac{5}{2}\right) \\ & + b\left(x - \frac{1}{2}, y - \frac{7}{2}\right) + b\left(x - \frac{1}{2}, y - \frac{9}{2}\right) + b\left(x - \frac{1}{2}, y - \frac{11}{2}\right) \\ & + b\left(x - \frac{1}{2}, y - \frac{13}{2}\right) + b\left(x - \frac{3}{2}, y - \frac{13}{2}\right) + b\left(x - \frac{5}{2}, y - \frac{13}{2}\right) \\ & + b\left(x - \frac{7}{2}, y - \frac{13}{2}\right) + b\left(x - \frac{9}{2}, y - \frac{13}{2}\right) + b\left(x - \frac{3}{2}, y - \frac{7}{2}\right) \\ & + b\left(x - \frac{5}{2}, y - \frac{7}{2}\right) + b\left(x - \frac{7}{2}, y - \frac{7}{2}\right), \end{aligned} \quad (16)$$

where b is the box function. These fourteen boxes form a block letter F , as shown in Figure 16. We compute the Radon projections of f using (16)

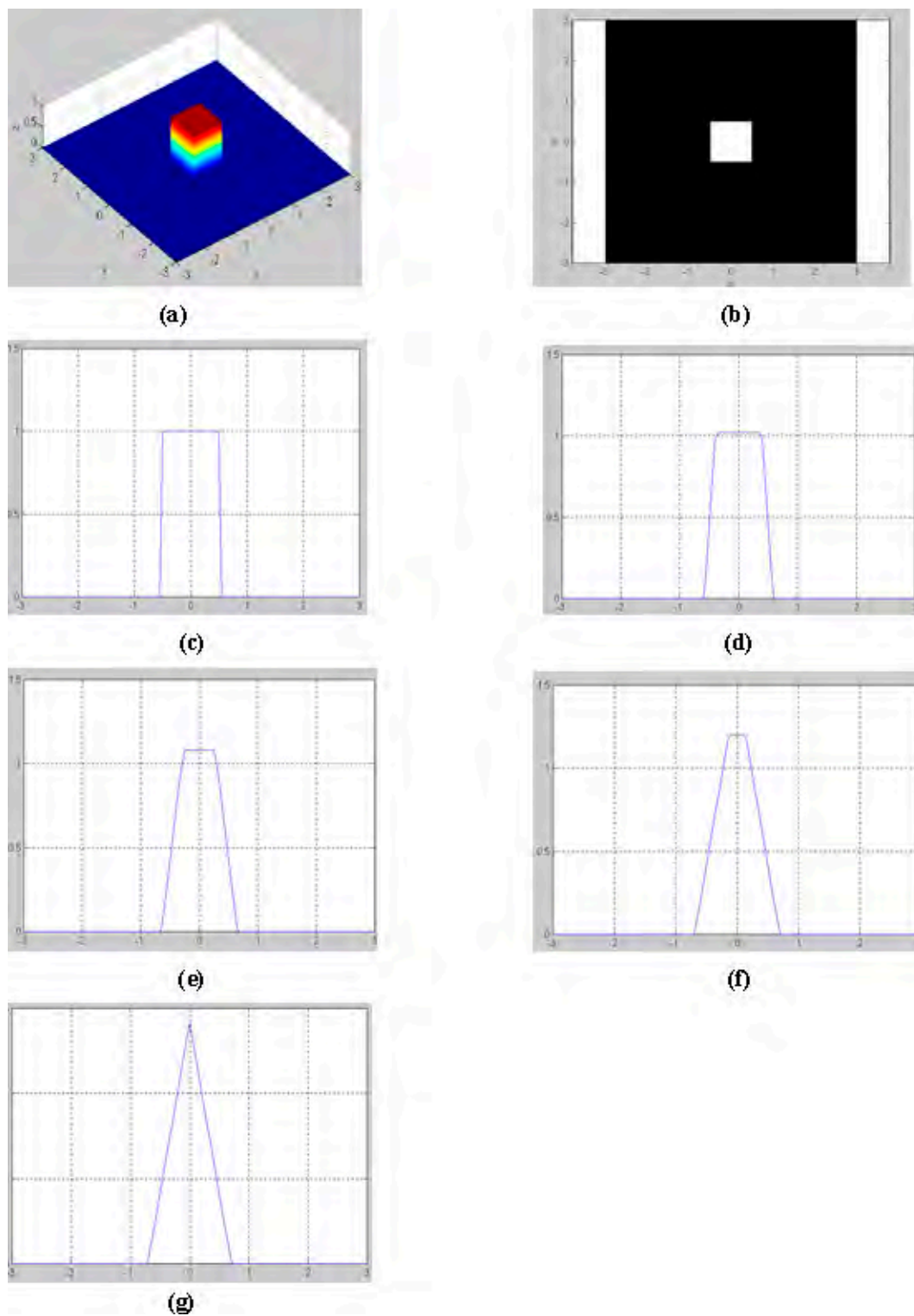


Figure 15. Representations of the unit box by a surface (a), by a density plot (a), and the profiles f_0^\vee , $f_{\pi/16}^\vee$, $f_{\pi/8}^\vee$, $f_{3\pi/16}^\vee$, and $f_{\pi/4}^\vee$ (c)–(g).

along with linearity and translation rules. Let

$$\begin{aligned}
 p_1 &= 0.5 \cos(\phi) + 0.5 \sin(\phi), & p_8 &= 1.5 \cos(\phi) + 6.5 \sin(\phi), \\
 p_2 &= 0.5 \cos(\phi) + 1.5 \sin(\phi), & p_9 &= 2.5 \cos(\phi) + 6.5 \sin(\phi), \\
 p_3 &= 0.5 \cos(\phi) + 2.5 \sin(\phi), & p_{10} &= 3.5 \cos(\phi) + 6.5 \sin(\phi), \\
 p_4 &= 0.5 \cos(\phi) + 3.5 \sin(\phi), & p_{11} &= 4.5 \cos(\phi) + 6.5 \sin(\phi), \\
 p_5 &= 0.5 \cos(\phi) + 4.5 \sin(\phi), & p_{12} &= 1.5 \cos(\phi) + 3.5 \sin(\phi), \\
 p_6 &= 0.5 \cos(\phi) + 5.5 \sin(\phi), & p_{13} &= 2.5 \cos(\phi) + 3.5 \sin(\phi), \\
 p_7 &= 0.5 \cos(\phi) + 6.5 \sin(\phi), & p_{14} &= 3.5 \cos(\phi) + 3.5 \sin(\phi),
 \end{aligned}$$

be the shift parameters $x_0 \cos \phi + y_0 \sin \phi$ from the translation rule (13) that correspond to the boxes from (16). We can then write

$$f^\vee(p, \phi) = \sum_{m=1}^{14} b_\phi^\vee(p - p_m).$$

Figure 16 shows representations of (16) by a surface, by a density plot, and by several projections.

Exercise

8. Consider the radially symmetric unit Gaussian

$$f(x, y) := e^{-\pi(x^2+y^2)}$$

that you worked in Exercise 5. Prove that $f_\phi^\vee(p) = e^{-\pi p^2}$. Plot $f_\phi^\vee(p)$.

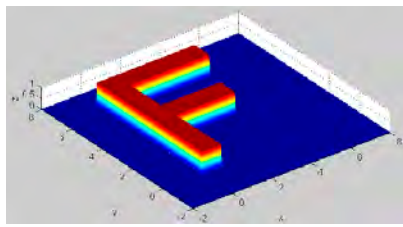
8. Reconstruction

In 1917, Radon gave the following inversion formula [Shepp and Kruskal 1978]. Assume that the projections $f^\vee\{L\}$ are given for all lines L , where f is continuous with compact support. If Q is any point in the plane, denote by $F_Q(q)$ the average value of $f^\vee\{L\}$ over all lines at distance $q > 0$. Then f is reconstructed by

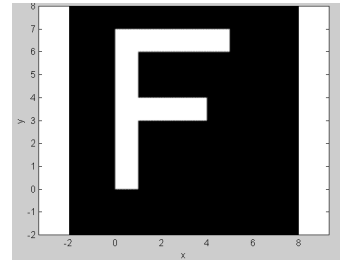
$$f(Q) = -\frac{1}{\pi} \int_0^\infty \frac{dF_Q(q)}{q}, \tag{17}$$

where this integral converges as a Stieltjes integral.

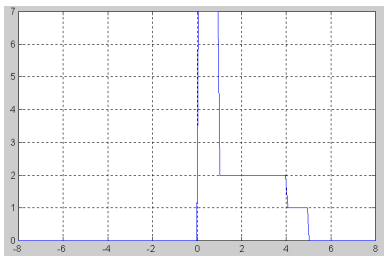
This pure mathematics result is fundamental to the problem of reconstruction. However, an inversion formula is not enough. Radon’s work assumes knowledge of the projections for infinitely many lines L . In practice, however, we work with a finite number of projections, and the determination of f from



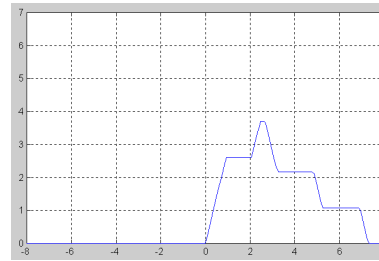
(a)



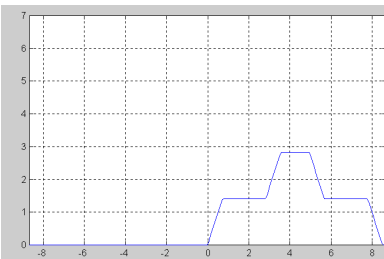
(b)



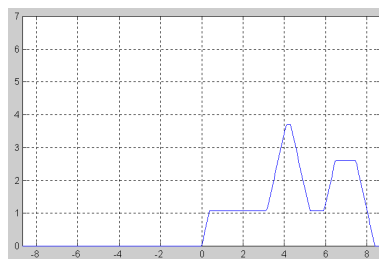
(c)



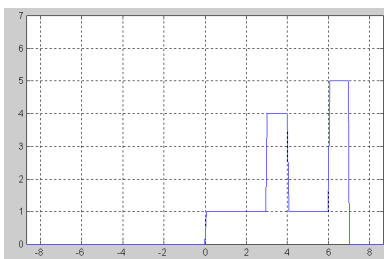
(d)



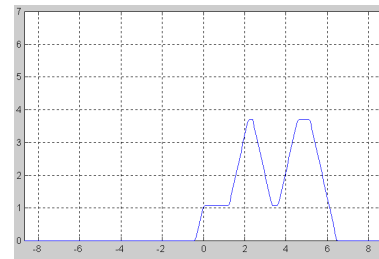
(e)



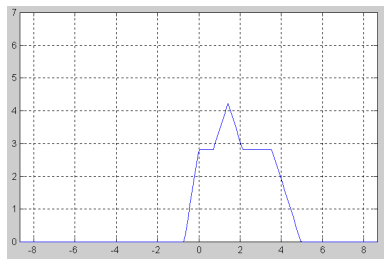
(f)



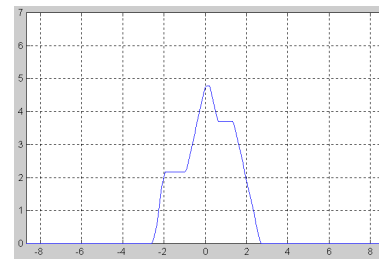
(g)



(h)



(i)



(j)

Figure 16. Representation of the letter F as a surface (a), as a density plot (b), and by the profiles f_ϕ^V for $\phi = 0, \frac{\pi}{8}, \frac{\pi}{4}, \frac{3\pi}{8}, \frac{\pi}{2}, \frac{5\pi}{8}, \frac{3\pi}{4},$ and $\frac{7\pi}{8}$ (c)–(j).

the set of projections f_ϕ^\vee is indeed an approximation. Also, the discrete approximations of (17) do not provide good reconstruction and typically lead to difficult questions [Shepp and Kruskal 1978].

The relation between the Radon transform and the Fourier transform will become clear in **Section 10**. The link between the two transforms goes back at least to Cramér and Wold in 1936 [Deans 1983; Shepp and Kruskal 1978].

Many mathematical approaches have been used for reconstruction, such as

- *back projection*, a crude but important method used in early experiments; and
- *filtered back projection*, which is an analytic method based on exact mathematical solutions and is used in commercial x-ray scanners.

In the context of the medical field, $f(x, y)$ corresponds to the density of tissue at a point (x, y) in some plane slice through a human body, and $f^\vee\{L\}$ is a measure of the logarithm of the absorption of an x-ray beam that passes through the body along line L . We measure a number of projections $f^\vee\{L\}$ and use them to synthesize the tissue density function f and display the corresponding image of a slice of the body. These mathematical ideas are used for magnetic resonance imaging (MRI) as well as for computed tomography (CT) images.

In the remainder of this section, we describe the back projection method. In **Section 10**, we present filtered back projection.

8.1 An Old Idea (Back Projection)

Back projection is a way of recovering $f(x, y)$ from its profiles f_ϕ^\vee . In practice, this method is not used, because it produces only a rough approximation of $f(x, y)$. However, by mastering the mathematics in this method, you will gain a key to the entire subject.

We consider again the cylinder function, as an opening example:

$$f(x, y) := \begin{cases} 1, & \text{if } x^2 + y^2 \leq \left(\frac{1}{2}\right)^2; \\ 0, & \text{otherwise.} \end{cases}$$

We have already explored this function and its profiles in **Examples 5** and **6**. As suggested in **Figure 17**, if we add up the effect of spreading each projection *back* across the image space, we would obtain a blurred rough image of the function $f(x, y)$. In particular, notice that the center of the image $(0, 0)$ receives a contribution from every profile.

For further illustration, consider **Figure 18**. The support of a function $f(x, y)$ is shown along with one profile f_ϕ^\vee that corresponds to an angle ϕ . You should contemplate this figure until you see how the point (x, y) , $f(x, y)$, ϕ , p , and f_ϕ^\vee are all related through this figure.

We would like to see the contribution that this single profile f_ϕ^\vee makes in estimating $f(x, y)$. We write

$$\begin{aligned} (\text{Backproj}f_\phi^\vee)(x, y) &:= f_\phi^\vee(p) \\ &= f_\phi^\vee(x \cos \phi + y \sin \phi). \end{aligned}$$

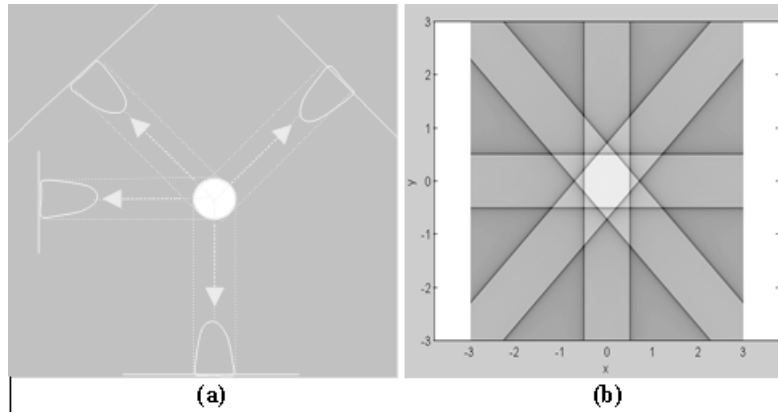


Figure 17. (Back projection) Spread each projection back across the plane.

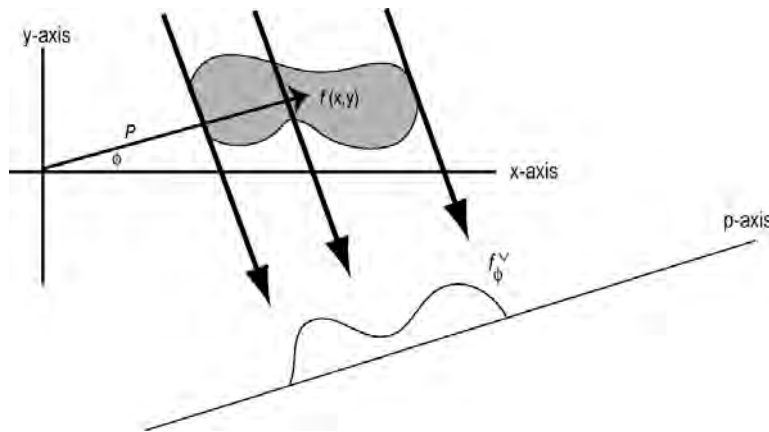


Figure 18. A function $f(x, y)$, and a profile $f_\phi^v(p)$.

In other words, $(\text{Backproj}f_\phi^v)$ maps the one dimensional profile, f_ϕ^v , to the function of two variables (x, y) that has constant values along the line $p = x \cos \phi + y \sin \phi$.

If f has compact support, then $(\text{Backproj}f_\phi^v)(x, y)$ is a band in the xy -plane that is orthogonal to the ray determined by ϕ , as illustrated in **Figure 19**.

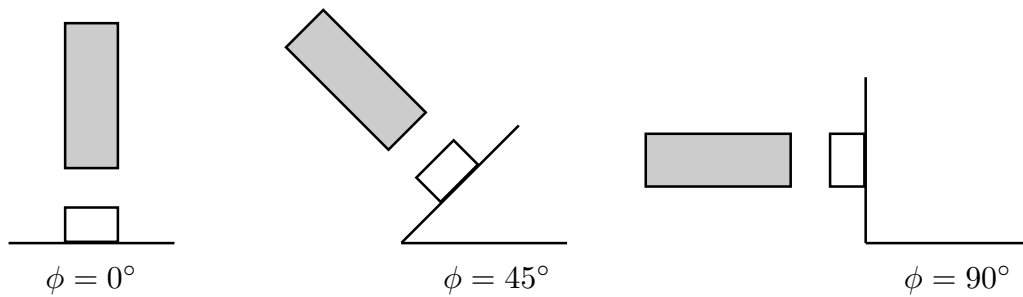


Figure 19. Back projection of the box function at angles $\phi = 0^\circ$, $\phi = 45^\circ$, $\phi = 90^\circ$.

To approximate the function $f(x, y)$ by a function $f_B(x, y)$, using all possi-

ble projections f_ϕ^\vee , we spread each projection back across the xy -plane. More precisely, we form f_B by accumulating back projections. Mathematically, we write [Deans 1983]

$$f(x, y) \approx f_B(x, y) := \int_{\phi=0}^{\pi} f_\phi^\vee(x \cos \phi + y \sin \phi) d\phi. \quad (18)$$

In practice, we replace the integral (18) by a corresponding discrete approximation

$$f_{B,N}(x, y) := \frac{\pi}{N} \sum_{m=0}^{N-1} f_{m\pi/N}^\vee \left[x \cos \left(\frac{m\pi}{N} \right) + y \sin \left(\frac{m\pi}{N} \right) \right]. \quad (19)$$

Example 9: Testing the ideas To test these ideas, pick one of the elementary functions introduced in **Examples 6–8**, say the cylinder function in **Example 6**, and do the following:

a) Write two Matlab codes, `codeA.m` and `codeB.m`, that implement the following formulas:

`codeA`: This function computes the cylinder function given in equation (10). So it takes (x, y) and returns $f(x, y)$.

`codeB`: This function computes projections $f_\phi^\vee(p)$ in equation (14). So it takes p and ϕ , and returns $f_\phi^\vee(p)$.

b) Write a script Matlab file (a driver) whose output is the following:

i. Display $[-3, 3] \times [-3, 3]$ image (a density plot) of the cylinder function. In this part you will call `codeA`.

ii. Display a plot for $f_\phi^\vee(p)$, by calling `codeB`.

iii. Display back projection images by implementing equation (19):

$$f_{B,N}(x, y) = \frac{\pi}{N} \sum_{m=0}^{N-1} f_{m\pi/N}^\vee \left[x \cos \left(\frac{m\pi}{N} \right) + y \sin \left(\frac{m\pi}{N} \right) \right],$$

with f_ϕ^\vee computed by calling `codeB`; the value for N is your choice. **Figure 20** shows plots for $f_{B,N}$ with $N = 1, 2, 4, 8, 16, 32,$ and 64 .

The image in (18) or (19) obtained by accumulating back projections is blurred, as illustrated in **Figure 20**. We discuss this issue and derive an exact formula in **Section 10**.

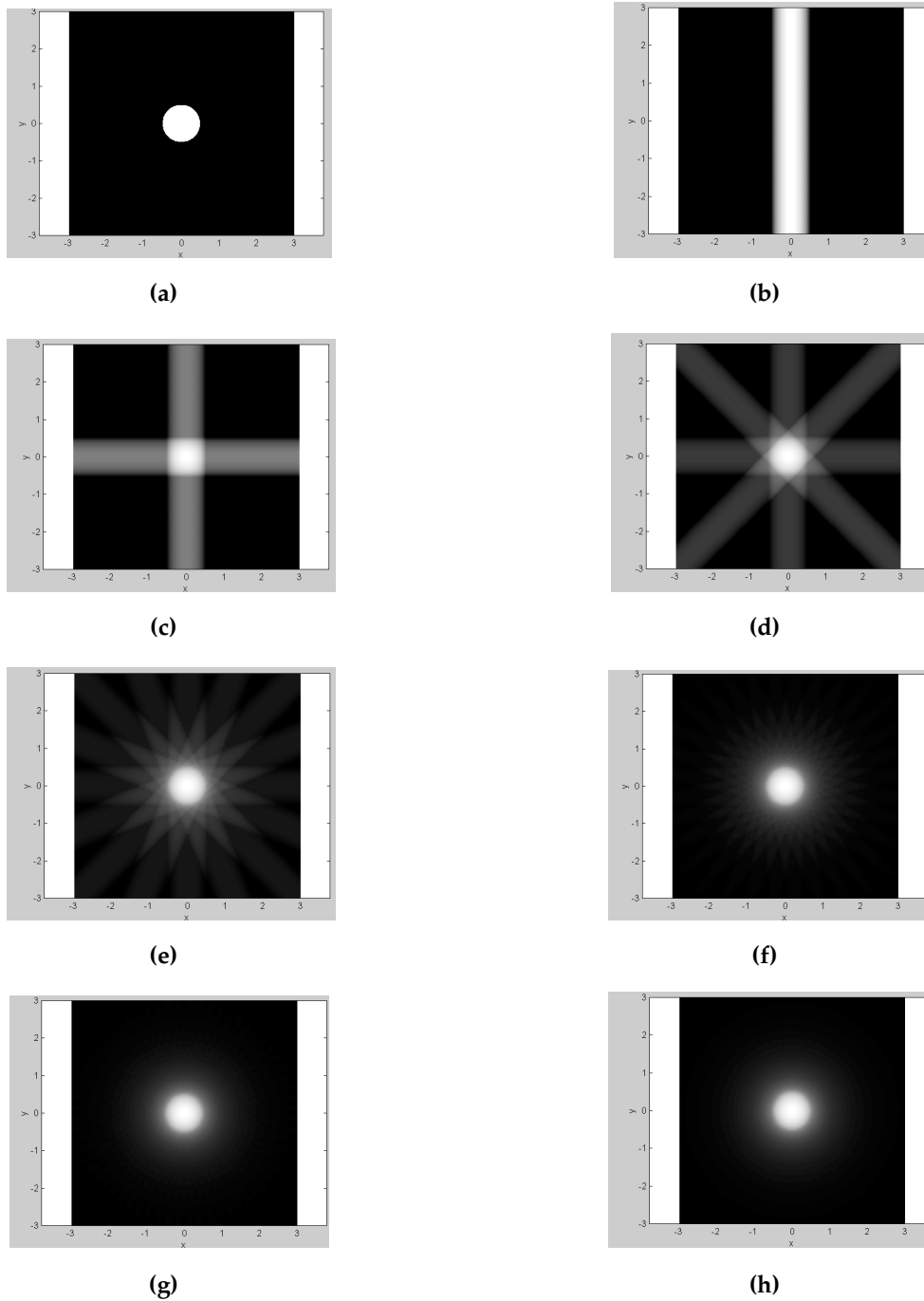


Figure 20. Density plots of the unit cylinder and the corresponding back projection images $f_{B,N}$, $N = 1, 2, 4, 8, 16, 32, 64$.

9. A Glimpse of Computed Tomography

In this section, we develop a brief analysis of the efforts that won the Nobel Prize in the subject. To see what computed tomography (CT) is, consider **Figure 21**, where we think of the xy -plane as a slice or layer under examination.

Points within the slice are described by a fixed coordinate system (x, y) , rays L (dashed line) are specified by p, ϕ as in (2). We may imagine a thin slice, say through the head, perpendicular to the main body axis. Several hundred parallel x-ray pencil beams are projected through the head in the plane of this slice.

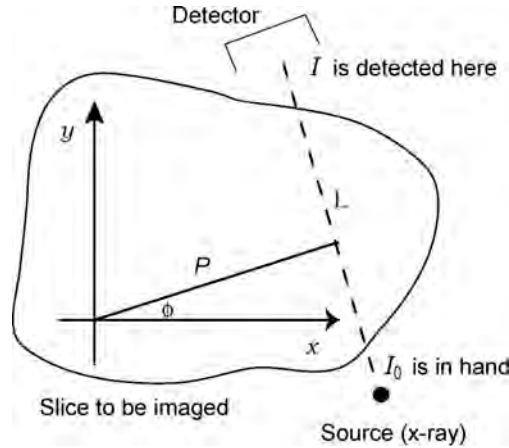


Figure 21. Coordinate systems. The density function is described with $x - y$ coordinates, $f(x, y)$. Rays are specified by their angle with the x -axis, ϕ and their distance from the origin, p .

The ray (line) L is characterized by the two numbers:

- I_0 = Input Intensity (number of photons per second per unit cross sectional area), and
- I = observed intensity after the beam passes through the object.

Observe that $I \leq I_0$, due to the absorption of the x-ray traveling through the object.

Let $f(x, y)$ = attenuation coefficient that depends on the density of the material [Deans 1983].

Physics proves that:

$$\begin{aligned}
 -\log\left(\frac{I}{I_0}\right) &= \int_L f(x, y) ds \\
 &= f_\phi^\vee(p).
 \end{aligned}
 \tag{20}$$

Since I_0 is in hand, and I can be detected, the left side of (20) can be computed. In this way, we can collect data to determine f_ϕ^\vee for as many angles ϕ as we wish. Having the profiles f_ϕ^\vee of the unknown (unseen) $f(x, y)$, we can use our mathematical tools to reconstruct $f(x, y)$ and display the image.

The British engineer Dr. Godfrey Hounsfield invented the first practical CT scanner in 1971. Hounsfield and the American physicist, Dr. A.M. Cormack, shared the Nobel prize in medicine and physiology in 1979 for their contribution in this field [Seeram 1994]. We emphasize one more time that the

fundamental principle behind this extraordinary invention is the mathematics of reconstruction.

We saw in **Section 3** that conventional imaging is conducted by simply forming shadows on a film, which is fundamentally Roentgen's invention. On the other hand, the CT approach gives the ability to view a body section or layer clearly without interfering with other regions; of course, a computer is needed to reconstruct and display the image $f(x, y)$ after the family f_ϕ^\vee is detected. **Figure 5** in **Section 3** illustrates a quick comparison. In **Figure 22**, we display a picture of a modern CT scan examination.



Figure 22. CT scan examination. (Image courtesy of St. John Health, <http://www.stjohn.org>.)

10. Filtered Back Projection

Back projection (18) produces a rough, blurred image with high density in the center due to the fact that many different images are overlapped there. However, back projection can be made to work if the profiles are in some way modified or filtered before being back-projected. In this section, we present a full derivation of what is known as *Fourier filtering*.

We begin by introducing the following important rule. Let

$$F(u, v) := \int_{-\infty}^{\infty} \int_{-\infty}^{\infty} f(x, y) e^{-2\pi i(ux+vy)} dx dy \quad (21)$$

be the two-dimensional Fourier transform of f . Let the univariate function

$$G_\phi(w) := F(w \cos \phi, w \sin \phi), \quad -\infty < w < \infty,$$

be the slice through F at the angle ϕ , and let $g_\phi(p)$ be the function with the

synthetic equation

$$g_\phi(p) = \int_{-\infty}^{\infty} G_\phi(w) e^{2\pi i w p} dw.$$

Then

$$f_\phi^\vee(p) = g_\phi(p), \quad (22)$$

or equivalently,

$$(\mathcal{F} f_\phi^\vee)(w) = F(w \cos \phi, w \sin \phi), \quad (23)$$

where \mathcal{F} is the univariate Fourier transform operator. Equation (23) is called the *projection slice rule*. It establishes the relation between the Radon transform and the Fourier transform.

We now introduce the polar coordinates

$$u = w \cos \phi, \quad v = w \sin \phi$$

in the Fourier synthesis equation

$$f(x, y) = \int_{-\infty}^{\infty} \int_{-\infty}^{\infty} F(u, v) e^{2\pi i (ux + vy)} du dv$$

with F given by (21). We thereby obtain

$$f(x, y) = \int_{\phi=0}^{2\pi} \int_{w=0}^{\infty} w F(w \cos \phi, w \sin \phi) e^{2\pi i w (x \cos \phi + y \sin \phi)} dw d\phi$$

and split this integral into the sum of I_1 and I_2 , with

$$\begin{aligned} I_1 &= \int_{\phi=0}^{\pi} \int_{w=0}^{\infty} w F(w \cos \phi, w \sin \phi) e^{2\pi i w (x \cos \phi + y \sin \phi)} dw d\phi, \\ I_2 &= \int_{\phi=\pi}^{2\pi} \int_{w=0}^{\infty} w F(w \cos \phi, w \sin \phi) e^{2\pi i w (x \cos \phi + y \sin \phi)} dw d\phi. \end{aligned}$$

We change the limits of the second integral by writing

$$\begin{aligned} I_2 &= \int_{\theta=0}^{\pi} \int_{w=0}^{\infty} w F(w \cos(\theta + \pi), w \sin(\theta + \pi)) e^{2\pi i w (x \cos(\theta + \pi) + y \sin(\theta + \pi))} dw d\theta \\ &= \int_{\theta=0}^{\pi} \int_{w=0}^{\infty} w F(-w \cos \theta, -w \sin \theta) e^{-2\pi i w (x \cos \theta + y \sin \theta)} dw d\theta \\ &= \int_{\theta=0}^{\pi} \int_{w=-\infty}^0 |w| F(w \cos \theta, w \sin \theta) e^{2\pi i w (x \cos \theta + y \sin \theta)} dw d\theta. \end{aligned}$$

We combine this expression for I_2 with that given above for I_1 to obtain

$$f(x, y) = \int_{\phi=0}^{\pi} \int_{w=-\infty}^{\infty} |w| F(w \cos \phi, w \sin \phi) e^{2\pi i w (x \cos \phi + y \sin \phi)} dw d\phi.$$

Finally, we use the projection slice rule (23) to rewrite this integral in the form

$$f(x, y) = \int_{\phi=0}^{\pi} \int_{w=-\infty}^{\infty} |w| (\mathcal{F} f_{\phi}^{\vee})(w) e^{2\pi i w (x \cos \phi + y \sin \phi)} dw d\phi.$$

In this way, we obtain the synthesis equation

$$f(x, y) = \int_{\phi=0}^{\pi} f_{\phi}^*(x \cos \phi, +y \sin \phi) d\phi \quad (24)$$

where

$$f_{\phi}^*(p) := \int_{w=-\infty}^{\infty} |w| (\mathcal{F} f_{\phi}^{\vee})(w) e^{2\pi i w p} dw. \quad (25)$$

In the early history of tomography, it was discovered that blurred representations of f could be obtained by using formula (18), as illustrated in Figure 20; but (24) shows that it is possible to produce the exact image f by accumulating back projections of f_{ϕ}^* . This accumulation has the effect of suppressing low-frequency components and enhancing high-frequency components that are needed to present edges. We say that f_{ϕ}^* is obtained by *filtering* f_{ϕ}^{\vee} and we refer to $f_{\phi}^*(x \cos \phi + y \sin \phi)$ as the *filtered back projection* of f_{ϕ}^{\vee} in the direction of ϕ . We use the discretization

$$f_{F,N}(x, y) := \frac{\pi}{N} \sum_{m=0}^{N-1} f_{m\pi/N}^* \left[x \cos \left(\frac{m\pi}{N} \right) + y \sin \left(\frac{m\pi}{N} \right) \right] \quad (26)$$

to approximate $f(x, y)$ by a finite sum of filtered back projections.

Example 10: Filtered back projection of the unit cylinder When f is the radial symmetric unit cylinder (10), we find in turn

$$\begin{aligned} f_{\phi}^{\vee}(p) &= \begin{cases} \sqrt{1 - 4p^2}, & \text{if } |p| \leq \frac{1}{2}; \\ 0, & \text{otherwise,} \end{cases} \quad (\mathcal{F} f_{\phi}^{\vee})(w) = \frac{1}{2} \frac{J_1(\pi w)}{w}, \\ (\mathcal{F} f_{\phi}^*)(w) &= |w| (\mathcal{F} f_{\phi}^{\vee})(w) = \frac{|w| J_1(\pi w)}{2w} \quad \text{and} \\ f_{\phi}^*(p) &= \int_{w=-\infty}^{\infty} \frac{|w| J_1(\pi w)}{2w} e^{2\pi i w p} dw \\ &= \int_{w=0}^{\infty} J_1(\pi w) \cos(2\pi w p) dw, \end{aligned} \quad (27)$$

where J_k is the Bessel function of the first kind of order k [Kammler 2000].

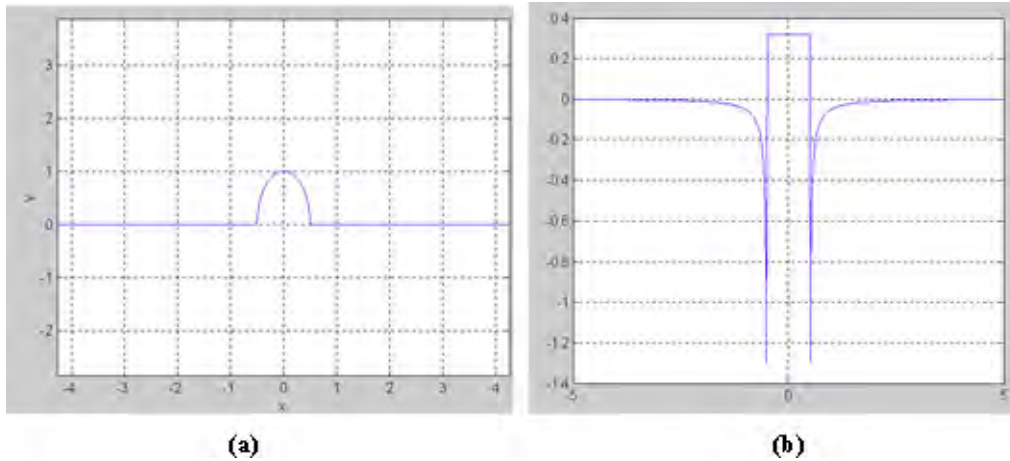


Figure 23. A profile (a) and a filtered profile (b) for the unit cylinder.

Figure 23 shows graphs of f_ϕ^\vee , f_ϕ^* for the unit cylinder function. Recall that f_ϕ^\vee for this particular function does not depend on ϕ , because of symmetry. Using formula (26) with f^* as in equation (27), you can display filtered back projection images for the cylinder function. Figure 24 shows the images $f_{F,N}$ with $N = 1, 2, 34, 8, 16, 32, 64$; compare this figure with Figure 20.

We conclude this section with two important remarks.

- Equation (25), which is known as *Fourier filtering*, is fundamental but needs further work before it can be used. Although we can successfully compute $f_\phi^*(p)$ for some elementary functions, such as equation (27) for the radial symmetric unit cylinder, that is just a nice “classroom” example that helps us test our ideas.

The presence of $|w|$ in equation (25) involves difficult questions, and this equation needs to be put in algorithmic context. Bracewell in 1965 was the first to work on this problem; he gave a widely-used alternative formula known as *convolution filtering*. Many others, such as Ramachandran and Lakshminarayanan provided further enhancing in convolution filtering [Shepp and Kruskal 1978]. Today many convolution algorithms are available, and all are included in the term “filtered back projection.” Interested students can conduct further research in Bracewell [1986], Brooks [1985], and Liang and Lauterbur [1999].

- We bring to the reader’s attention two approximations needed when using filtered back projection in applications, regardless of the particular filtering algorithm used:
 - Replacement of the integral by summation, as we did in (26).
 - Because for a given angle ϕ , $f_\phi^*(p)$ is calculated in only a discrete form, interpolation is needed to find $f_\phi^*(p)$ at an arbitrary p .

Exercise

9. In this exercise, you will learn the basics of another reconstruction method, which does not use back projection, known as *two-dimensional Fourier reconstruction*.
 - a) Begin with equation (23), which shows the link between the Radon and Fourier transforms. Explain this relation using your own words. How can this equation be used to reconstruct $f(x, y)$ from f_ϕ^\vee ?
 - b) In **Exercise 8**, you proved that the Radon transform of the radially symmetric Gaussian is given by $f_\phi^\vee(p) = e^{-\pi p^2}$. Apply (23) to recover the Gaussian from its Radon transform.

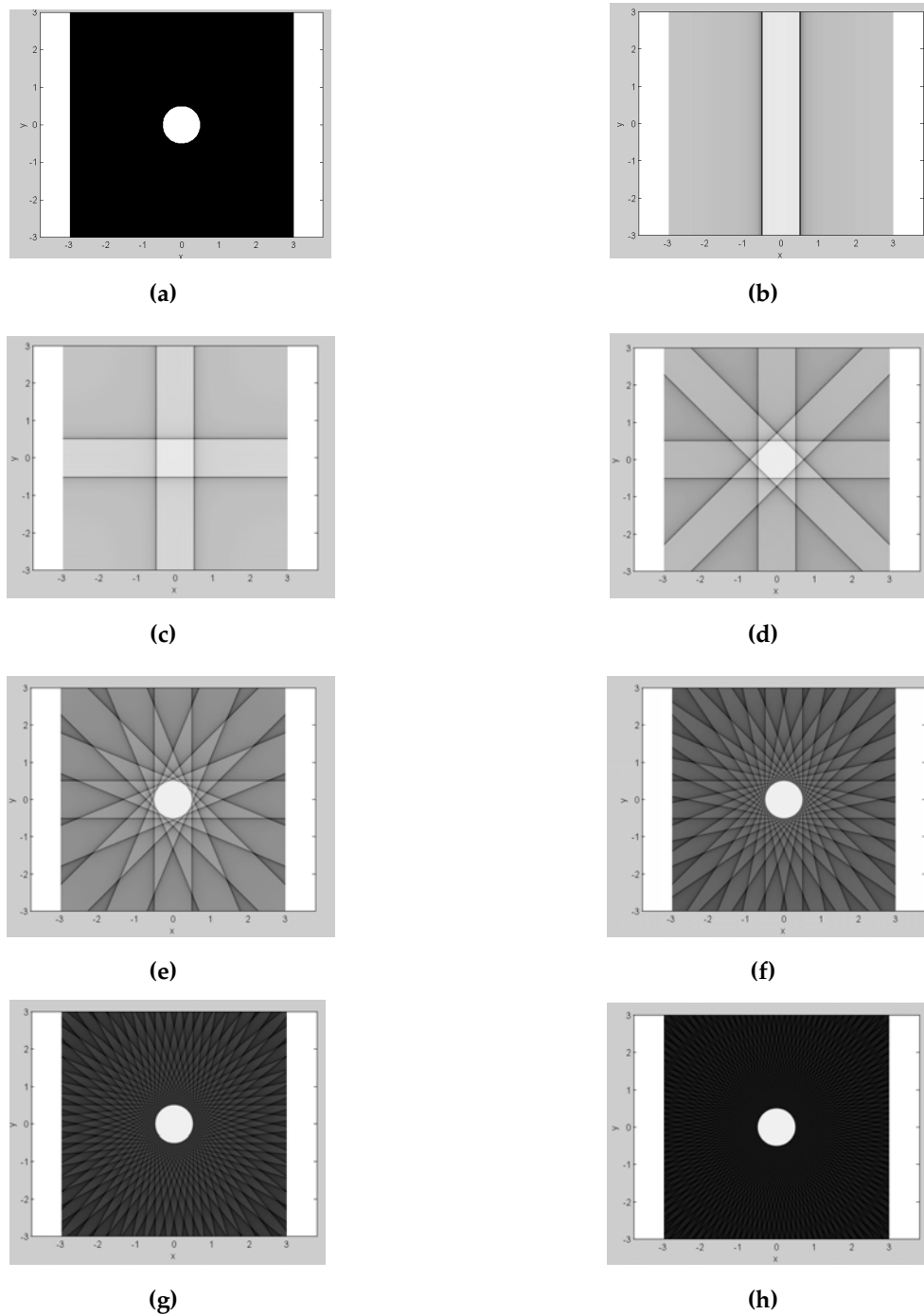


Figure 24. A density plot of the unit cylinder and corresponding density plots of the filtered back projected images (26) with $N = 1, 2, 4, 8, 16, 32, 64$ and f_ϕ^* as given in (27).

11. Matlab Project

When we dealt with the radial symmetric unit cylinder in **Example 10**, we implemented formula (26) combined with (27). Here, we discuss an example of recovering a function using some Matlab commands.

The Image Processing Toolbox in Matlab is a collection of functions that support a wide range of image processing operations. In particular, we briefly describe the following two functions.

- **radon**

This function computes the projection of an image matrix $f(x, y)$ along a specified direction. The command

```
[R, xp] = radon(I, theta);
```

computes the Radon transform of the image I for the angles specified in the vector `theta`. The columns of R contain the Radon transform for each angle in `theta`. The vector `xp` contains the corresponding coordinates along the p -axis.

- **iradon**

This function performs the inverse Radon transform, using the filtered back projection algorithm:

```
IR = iradon(R, theta);
```

In using Matlab commands, you need to be aware of the differences in scaling between our previous illustration and the scaling that results from Matlab functions. We recommend that you use the `help` command to display information in the Matlab Command Window.

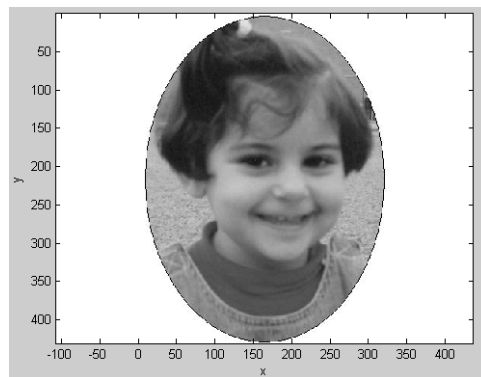
Study **Example 11** and then do **Exercise 10**, where you will recover an image of your choice.

Example 11: Grayscale images The images that we have used so far have all been binary images: $f(x, y)$ is either 1 or 0. In this example, we work with an image with different gray levels. We define

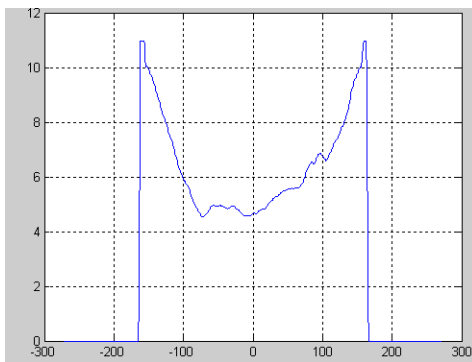
$$f(x, y) = \text{Sara}(x, y).$$

We scanned the original color version of the photo shown in **Figure 25a** and saved it as a JPEG image, calling it `MyImag`. Using Matlab, as shown in Code2 in **Table 2** on p. 36, we can:

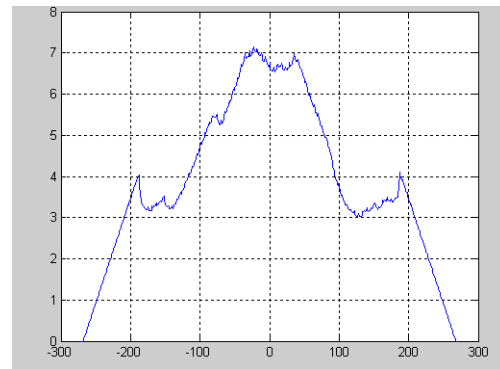
1. Display `MyImag` (**Figure 25a**), after using the Matlab command `gb2gray` to convert the image to grayscale, as shown in Code2.
2. Compute and save several projections of `MyImag`. Three projections, corresponding to $\phi = 0^\circ, 45^\circ$, and 90° , are shown in **Figure 25b–d**.
3. Compute and display several reconstructed images using the commands `radon` and `iradon` (**Figure 26**).



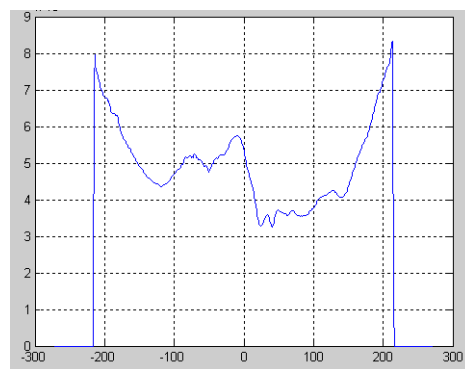
(a)



(b)

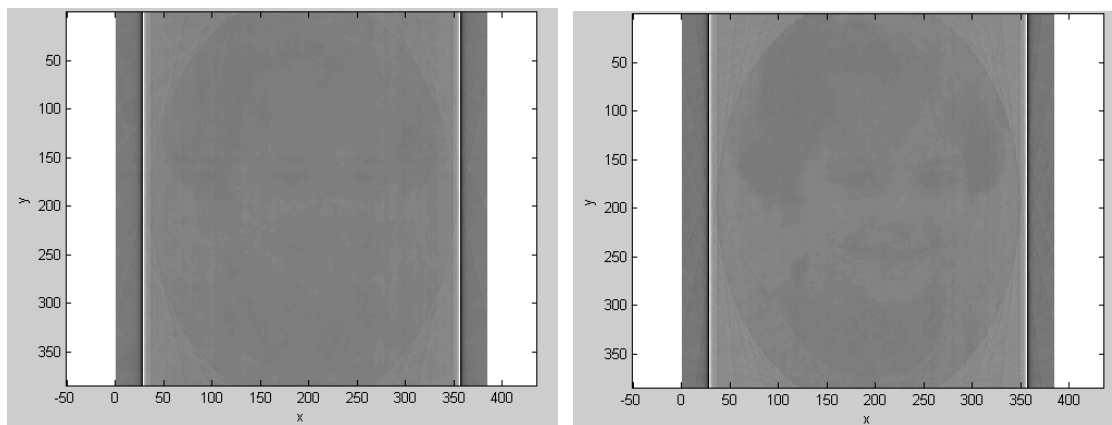


(c)



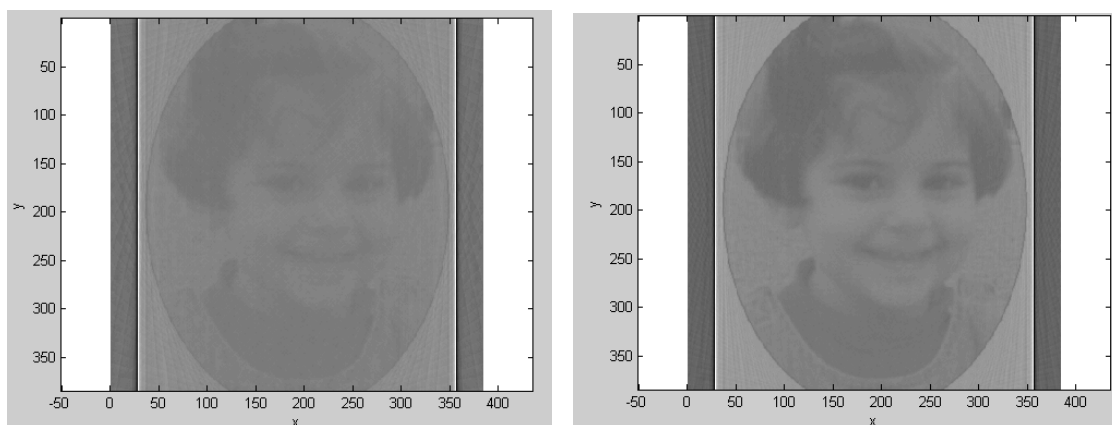
(d)

Figure 25. a. Original image, $Sara(x, y)$. b–d. Projections of Sara corresponding to angles 0° , 45° , and 90° , using the Matlab command `radon`.



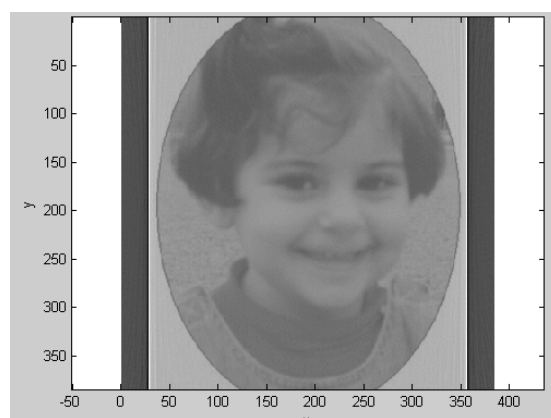
(a)

(b)



(c)

(d)



(e)

Figure 26. Filtered back projection of Sara using 15°, 30°, 45°, 90°, and 180° projections.

Exercise

10. Following the steps of **Example 11**, perform the same steps on a photo of your choice. Code2 in **Table 2** is one way of doing this exercise. You may study it and make changes, or you can just use it.

Table 2. Code2.

```

% Code2: a script MATLAB file;
% uses radon and iradon as explained in Example 11.

% Part1: Read and display the original image.
I = imread('MyImag','jpg'); % Read the original image 'MyImag'
                               % and save it as a matrix C
C = rgb2gray(I);             % Convert colormap to grayscale.
figure(1)
imagesc(C);                 % Display the image
colormap(gray);
shading interp
xlabel('x')
ylabel('y')
axis equal
title(' Figure(1) :Input MyImag')

% Part 2:compute and display projections
theta0= 0; % Note: You may change theta0 to any angle you want
[R0,xp0] = radon(C,theta0);
figure(2)
plot(xp0,R0),grid
title(' Figure(2) :The Zero Projection of MyImag ')

% Part 3: Practicing
% Here we use radon to collect profiles, and then we
%use iradon to get an image using these profiles.

theta =linspace(0,180,2);   % Here we use 90-degree projections, but by
                               % changing theta you can display different
                               % images.
                               % If theta is a vector,it must contain angles
                               % with equal spacing between them.

[R,xp] = radon(C,theta);
I = iradon(R,theta);
figure(3)
imagesc(I);
colormap(gray);
shading interp
xlabel('x')
ylabel('y')
axis equal
title(' Figure(3) :Filtered Back projection of MyImag Using 90 projections')

```

12. Solutions to the Exercises

1. You can use the script file Code3 in **Table S1**. The output is shown in **Figure S1**.

Table S1. Code3.

```

% Code3: a script MATLAB file;
% generates surface surface
% and density plots for the radially symmetric
% unit Gaussian.

step = .03;
s = -3:step:3;  t=s;

[A,B]= meshgrid(s,t);          % define a grid
C = zeros(length(s),length(s));
for i=1:length(s)
for j=1:length(t)
    x=A(i,j);
    y=B(i,j);
    C(i,j)=exp(-(x^2+y^2));
end
end
figure(1)
surf(A,B,C)                    % display the surface
view([20,20,120])
shading interp
xlabel('x')
ylabel('y')
zlabel('z')
title('Surface of the Gaussian Function')

figure(2)
pcolor(A,B,C)                  % display the image
colormap(gray);
shading interp
xlabel('x')
ylabel('y')
axis equal
title('Density Plot for the Gaussian Function')

```

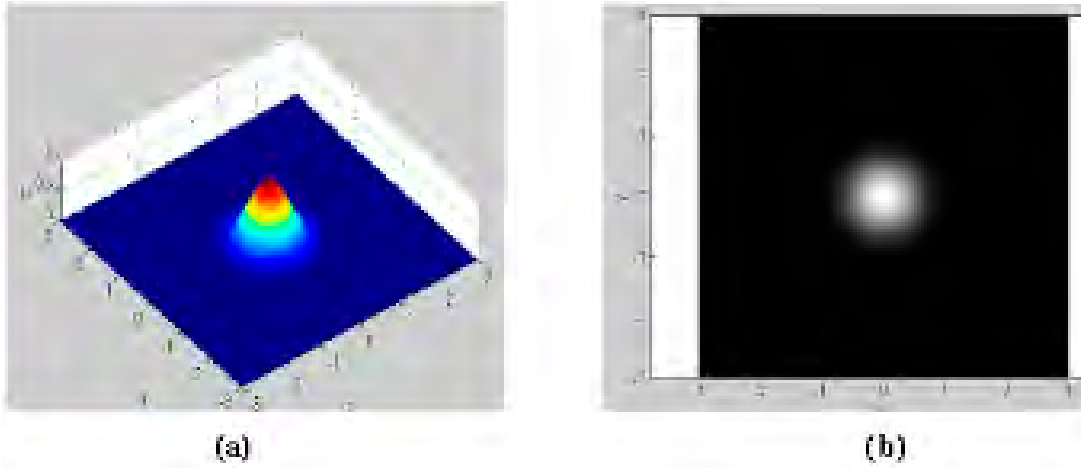


Figure S1. Representations of the radially symmetric unit Gaussian by a surface **(a)** and by a density plot **(b)**.

2. Let (x, y) be any point on L . The slope of L is

$$m := \frac{-\cos \phi}{\sin \phi}.$$

Also, L passes through the point $(p \cos \phi, p \sin \phi)$. Thus, the equation of L is

$$y - p \sin \phi = \frac{-\cos \phi}{\sin \phi} (x - p \cos \phi).$$

Now, solve for p .

$$\begin{aligned} 3. \quad F(s) &= \int_{x=-\infty}^{\infty} e^{-\pi x^2} e^{-2\pi i s x} dx \\ &= \int_{x=-\infty}^{\infty} e^{-\pi x^2} [\cos(2\pi s x) + i \sin(2\pi s x)] dx \\ &= \int_{x=-\infty}^{\infty} e^{-\pi x^2} \cos(2\pi s x) dx, \end{aligned}$$

since $e^{-\pi x^2}$ is even and the sin is odd. Now do the calculation.

$$\begin{aligned} 4. \quad F(u, v) &= \int_{x=-\infty}^{\infty} \int_{y=-\infty}^{\infty} f_1(x) \cdot f_2(y) e^{-2\pi i (ux+vy)} dy dx \\ &= \left\{ \int_{x=-\infty}^{\infty} f_1(x) e^{-2\pi i u x} dx \right\} \left\{ \int_{y=-\infty}^{\infty} f_2(y) e^{-2\pi i v y} dy \right\} \\ &= F_1(u) \cdot F_2(v). \end{aligned}$$

5. Apply the results of **Exercise 4** together with **Exercise 3**.
6. $f_0^\vee(p)$ is shown in **Figure S2**.

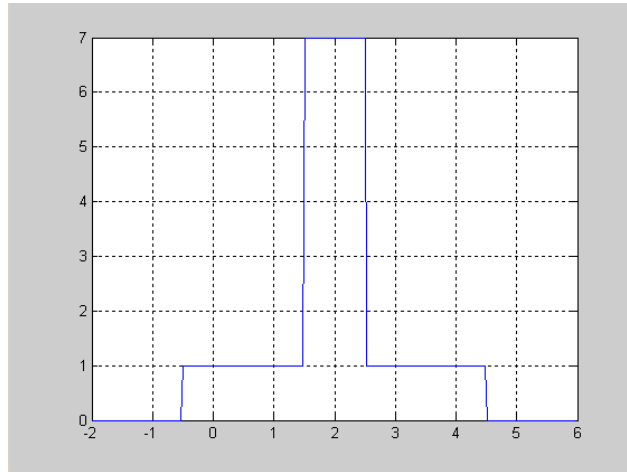


Figure S2. $f_0^\vee(p)$ for the T image.

7.

$$\begin{aligned} g_\phi^\vee(p) &= \int_L c_1 f_1(x, y) + c_2 f_2(x, y) ds \\ &= c_1 \int_L f_1(x, y) ds + c_2 \int_L f_2(x, y) ds. \end{aligned}$$

8. We have $f(x, y) := e^{-\pi(x^2+y^2)}$, which is radially symmetric, so we can use **(11)** to write

$$\begin{aligned} f_\phi^\vee(p) &= f_0^\vee(p) = \int_{-\infty}^{\infty} f(p, y) dy \\ &= \int_{-\infty}^{\infty} e^{-\pi(x^2+y^2)} dy \\ &= e^{-\pi p^2}. \end{aligned}$$

The resulting $f_0^\vee(p)$ is shown in **Figure S3**.

9. **a)** We say that the two-dimensional Fourier transform $F(u, v)$ of $f(x, y)$ may be obtained by a Radon transform f_ϕ^\vee followed by one-dimensional Fourier transform, here

$$u = w \cos \phi, \quad v = w \sin \phi, \quad \text{and} \quad w^2 = u^2 + v^2.$$

- b)** From **Exercise 8**, we have

$$f_\phi^\vee(p) = e^{-\pi p^2};$$

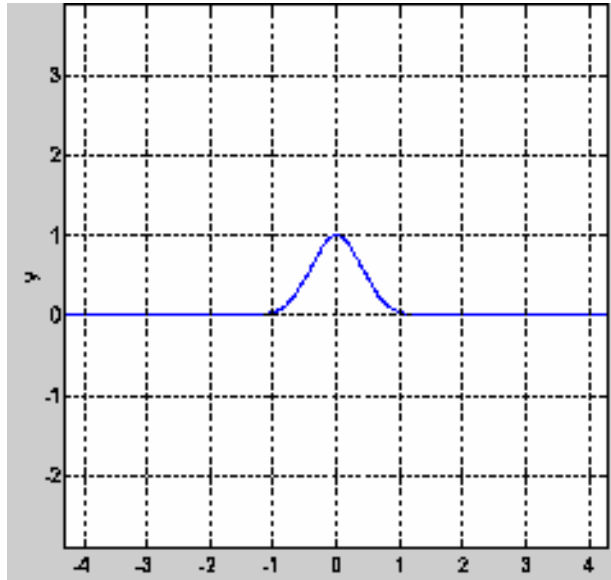


Figure S3. f_0^\vee of the radially symmetric unit Gaussian.

but by **Exercise 3**, we have

$$\mathcal{F}(f_\phi^\vee)(w) = e^{-\pi w^2}.$$

Applying **(23)**, we get

$$\begin{aligned} F(u, v) &= F(w \cos \phi, w \sin \phi) \\ &= e^{-\pi w^2} \\ &= e^{-\pi(u^2+v^2)}. \end{aligned}$$

This means that we can obtain $F(u, v)$ from f_ϕ^\vee . But then we can recover $f(x, y)$ from $F(u, v)$ by using **(7)**. Indeed, here $f(x, y)$ is the unit Gaussian, from **Exercise 5**.

References

- Kevles, Bettyann Holtzmann. 1997. *Naked to the Bone: Medical Imaging in the Twentieth Century*. New Brunswick, NJ: Rutgers University Press.
- Bracewell, R.N. 1986. *The Fourier Transform and Its Applications*. 2nd ed. New York; McGraw-Hill, 1986.
- Brooks, R.A., and G. Di Chiro. 1975. Theory of image reconstruction in computed tomography. *Radiology* 117: 561–572.
- Deans, S.R. 1983. *The Radon Transform and Some of Its Applications*. New York: John Wiley & Sons.
- Gonzales, R.C., and R.E. Woods. 2002. *Digital Image Processing*. 2nd ed. Reading, MA: Addison-Wesley.
- Kammler, D.W. 2000. *A First Course in Fourier Analysis*. Upper Saddle River, NJ: Prentice-Hall.
- Liang, Zhi-Peu, and Paul C. Lauterbur. 1999. *Principles of Magnetic Resonance Imaging*. New York: Wiley-IEEE Press.
- Seeram, Euclid. 1994. *Computed Tomography*. Philadelphia, PA: W.B Saunders.
- Shepp, L.A., and J.B. Kruskal. Computerized tomography: The new medical x-ray technology. *American Mathematical Monthly* 85 (1978) (6) 420–438.

About the Author



Dr. Hjouj has a bachelor's degree from Yarmouk University in Jordan, a master's degree from An-Najah National University in Palestine, and a Ph.D. from Southern Illinois University, all in mathematics. The Sara in the images in this Module is his daughter. Dr. Hjouj is teaching at East Carolina University and at Craven College in North Carolina.